

This dissertation has been 64-8833  
microfilmed exactly as received

HILCHIE, Douglas Walter, 1930-  
THE EFFECT OF PRESSURE AND TEMPERATURE  
ON THE RESISTIVITY OF ROCKS.

The University of Oklahoma, Ph.D., 1964  
Engineering, general

University Microfilms, Inc., Ann Arbor, Michigan

THE UNIVERSITY OF OKLAHOMA  
GRADUATE COLLEGE

THE EFFECT OF PRESSURE AND TEMPERATURE  
ON THE RESISTIVITY OF ROCKS

A DISSERTATION  
SUBMITTED TO THE GRADUATE FACULTY  
in partial fulfillment of the requirements for the  
degree of  
DOCTOR OF PHILOSOPHY

BY  
DOUGLAS W. HILCHIE  
Norman, Oklahoma  
1964

THE EFFECT OF PRESSURE AND TEMPERATURE  
ON THE RESISTIVITY OF ROCKS

APPROVED BY

Paul Campbell  
Arthur Bernhart  
Sheril D. Christian  
Ruston L. Moore  
John A. E. Norton

DISSERTATION COMMITTEE

## ABSTRACT

Six brine saturated porous samples were subjected to simulated overburden pressures up to 10,000 psi., simulated reservoir temperatures up to 400°F. and simulated reservoir conditions up to 10,000 psi. and 400°F. The effects of temperature and/or pressure on the resistivity of the samples were measured in a cell developed to facilitate this type of measurement on a routine basis.

The pressure tests indicated that the resistivity increased and the porosity decreased as the pressure was increased. All samples were found to have rapidly increasing resistivity as the initial pressures were applied. The rate of increase of resistivity decreased continually with the application of additional pressure with the exception of the Paradox (limestone) which increased almost linearly. The sensitivity of the resistivity increase was shown to be a function of the percent of pore volume represented by pores of radius less than 0.5 microns and the clay content.

The Formation Resistivity Factor went through a minimum and then increased as the temperature was increased and the net pressure held constant. The magnitude and temperature of the occurrence of the minimum varied with individual samples as well as the magnitude of the increase after the minimum. The effects could be predicted if the percent pore volume represented by the pores less than 0.5 microns and the temperature of the minimum were known.

The combined temperature and pressure increases caused the Formation Resistivity Factor to increase. In general the additive results of the separate temperature and pressure data were equal to the combined pressure-temperature experimental data at low and moderate temperatures.

## ACKNOWLEDGMENT

The author wishes to express his appreciation to Dr. J. M. Campbell, who supervised this study, for his constructive criticisms and careful review of this manuscript.

Financial support from the Socony Mobil Oil Company, Incorporated is gratefully acknowledged.

Finally, the author thanks all the people who knowingly or unknowingly helped make this dissertation possible.

## TABLE OF CONTENTS

	Page
ABSTRACT . . . . .	iii
ACKNOWLEDGMENT . . . . .	v
LIST OF TABLES . . . . .	vii
LIST OF ILLUSTRATIONS. . . . .	viii
<b>Chapter</b>	
I. INTRODUCTION . . . . .	1
II. THEORY . . . . .	8
III. PROCEDURE OF INVESTIGATION . . . . .	16
IV. DISCUSSION OF THE DATA ACCURACY. . . . .	37
V. RESULTS AND ANALYSIS OF DATA . . . . .	39
VI. CONCLUSIONS . . . . .	80
<b>APPENDICES</b>	
A. SAMPLE DESCRIPTIONS . . . . .	82
B. EXPERIMENTAL DATA . . . . .	84
BIBLIOGRAPHY . . . . .	96

## LIST OF TABLES

Table	Page
I. Dimensions and Porosities of Samples . . . . .	18
II. X-Ray Diffraction Analyses of Sandstone Samples. . . . .	19
III. Summary of the Effects of Pressure . . . . .	52
IV. Comparison of Experimental and Calculated Relative Formation Resistivity Factors. . . . .	69
V. Volumetric Changes Due to Pressure . . . . .	85
VI. Resistivity Changes Due to Pressure. . . . .	88
VII. Resistivity Changes Due to Temperature . . . . .	91
VIII. Resistivity Changes Due to Pressure and Temperature. . .	94



## LIST OF ILLUSTRATIONS

Figure	Page
1. Formation Resistivity Factor versus Porosity for Constant Constriction Factor and Various Tortuosities . . . . .	11
2. Formation Resistivity Factor versus Porosity for Constant Tortuosity and Various Constriction Factors. . . . .	12
3. Comparison of Selected Formation Resistivity Factor-Porosity Relationships for Unconsolidated Sands. . . . .	14
4. The High Temperature and Pressure Cell Completely Assembled	21
5. High Temperature and Pressure Resistivity Cell . . . . .	22
6. Unassembled Core Assembly and Cell Top . . . . .	23
7. Schematic of Pressure Regulating System. . . . .	24
8. Oil-Water Warning System . . . . .	26
9. Schematic of Resistivity Measuring System. . . . .	30
10. The Effects of Overburden Pressure on Rock Resistivity . .	40
11. Comparison of Resistivity Data of Fatt, Glanville, Redmond, and Hilchie . . . . .	41
12. Mercury Injection Pore Size Distribution for Alundum . .	42
13. Mercury Injection Pore Size Distribution for Bandera . .	43
14. Mercury Injection Pore Size Distribution for Berea. . . .	44
15. Mercury Injection Pore Size Distribution for Briar Hill. .	45
16. Mercury Injection Pore Size Distribution for Dean . . . .	46
17. Mercury Injection Pore Size Distribution for Paradox. . .	47
18. Compressibility versus Relative Formation Resistivity Factor . . . . .	49

Figure	Page
19. Pore Volume $< .5$ Microns versus Relative Formation Resistivity Factor . . . . .	51
20. Clay Content versus Relative Resistivity . . . . .	54
21. Comparison of Data and Clay Content Correlation. . . . .	55
22. Comparison of Data and Pore Size Correlation . . . . .	57
23. The Change in "m" With Net Pressure. . . . .	58
24. Effect of Temperature on Relative Resistivity of Berea . .	61
25. Effect of Temperature on the Relative Resistivity of Paradox and Dean Samples. . . . .	62
26. Effect of Temperature on the Relative Resistivity of Briar Hill, Bandera, and Alundum. . . . .	63
27. Percent Pore Volume $< .5$ Microns versus Minimum $\frac{F^T}{F}$ . . .	65
28. Pore Volume $< .5$ Microns versus "A" . . . . .	66
29. "A" versus $\alpha$ . . . . .	67
30. Comparison of Data and Calculated Relative Formation Resistivity Factor for Briar Hill . . . . .	70
31. Comparison of Data and Calculated Relative Formation Resistivity Factor for Dean . . . . .	71
32. Comparison of Data and Calculated Relative Formation Resistivity Factor for Paradox. . . . .	72
33. Effects of Temperature Plus Pressure on Alundum. . . . .	74
34. Effects of Temperature Plus Pressure on Berea. . . . .	75
35. Effects of Temperature Plus Pressure on Briar Hill . . . . .	76
36. Effects of Temperature Plus Pressure on Bandera. . . . .	77
37. Effects of Temperature Plus Pressure on Paradox. . . . .	78

## CHAPTER I

### INTRODUCTION

The primary concern of this thesis is the effect of elevated temperatures and/or pressures on the electrical resistivity of porous-fluid saturated rocks. This property as well as the other physical and chemical properties of rocks is vitally important to our improved analysis of porous media behavior, particularly as wells tend to become deeper.

The electrical resistivity of rocks has traditionally been measured at atmospheric pressure and ambient temperature. This approach stems from a time when most wells were fairly shallow and methods of interpretation did not demand a rigorous analysis of these properties. It was generally recognized that removing the rock from its native environment, flushing it with the drilling fluid, and changing the temperature and pressure, would yield a rock that, at best, would bear only a partial resemblance property wise to its condition in the native state. Until recent years this problem has been largely ignored because of the relative difficulty of taking data under pressure and because the pressure and temperature changes encountered while cutting and testing a sample did not seem critical enough to cause obvious trouble. Furthermore, at least a portion of the discrepancy could be empirically removed by back-correlating rock behavior in place against its pseudo-properties obtained at atmospheric conditions.

Although it is widely recognized that rocks under high pressure and temperature become more "plastic" and are less "brittle" than at atmospheric conditions, little attention has been focused on the variation in properties that might accompany this change. This is somewhat surprising for the ability to accurately predict electrical resistivity, porosity, permeability, and compressibility under in-situ conditions plays a key role in many of our engineering calculations. Knowledge of these properties is vital to many aspects of electrical logging, fracturing, and many facets of the flow of fluids.

The electrical resistivity of rocks plays a key role in the interpretation of well logs for it is used as a basic parameter in the determination of porosity. This formation factor-porosity relationship serves as one of the cornerstones of logging theory. Although published data in this area are fairly meager, there have been some significant works on the effect of overburden pressure on electrical resistivity. However, no investigation has been reported pertaining to the effect of temperature (with or without pressure) on resistivity. It has been generally assumed that the resistivity of a porous media simply varies with temperature at the same rate as does the resistivity of the saturating fluid. Because data in this area are virtually non-existent but yet so critical, their development serves as a logical focal point for this work.

As later discussions will show, the problem is too complex for a study of this scope to completely solve. Although it has been feasible to develop a rigorous correlation on the relatively few rock samples tested, an important insight is provided into rock behavior that should be of real value. The results shown should not only "condition" our

present thinking but serve as a firm basis for future work. The development of a reliable experimental technique presented herein (which proved difficult) is in itself of importance.

The effect of temperature can be dramatic. Formation temperatures increase with burial depth. In general the increase is about 1°F. per 100 feet although many anomalies are noted. Sediments have been found with a temperature near freezing in the Arctic regions while in Southern Texas some temperatures exceed 400°F.

In view of the fact that the combination of rock lithology, pressure, and temperature actually encountered are virtually endless, it has only been possible to choose representative values of these parameters. To increase the immediate utility of the results, rocks with widely varying properties have been chosen.

#### PREVIOUS WORK

The studies reviewed in this paper are limited to those relating to the net pressure effects on the resistivity of rocks.

Fatt<sup>8</sup> determined the effect of both internal and external pressures up to 5000 psi. on the formation resistivity factor\* of 20 brine saturated sandstones. At elevated pressure it was about 35% above the atmospheric value. A comparison of the variation of porosity, resistivity, and permeability with increased overburden pressure indicated that the sensitivity of these parameters varied greatly,

---

\* Formation resistivity factor is the resistivity of a saturated rock divided by the resistivity of the saturating fluid.

with the permeability being the most sensitive, the porosity the least, and the electrical conductivity somewhere in between. One of the more important results of this work was that "the laboratory measured formation resistivity factors in which only the external pressure is varied are sufficient to give information of the effect of overburden pressure on the conductivity of porous rocks." This in effect says that it is possible to obtain good results in the laboratory using low internal pressures (instead of the natural fluid pressures) and equivalently reduced external pressures.

Wyble<sup>32</sup> reported the effects of 0-5000 psig. simulated overburden pressure on the conductivity of three sandstones. His experiments were conducted using the assumption that a radially applied pressure is the equivalent of the conditions experienced in the native environment. Generally it is believed that the stresses on the in-situ rocks are somewhere between the normally used 3 equal stresses and the case of a large vertical stress and small horizontal stresses. Wyble's assumption does not agree with the commonly accepted hypotheses mentioned above, but no experimental evidence is available to indicate the degree of error (if any) this assumption creates. The results of this study generally agree with those of other investigators.

Glanville<sup>11</sup> published the effect of pressure on the resistivity of two sandstones and three carbonates. Effective stresses up to 5000 psi. were used and little or no difference was found on the effects of pressure on the vertical and horizontal resistivities.

Redmond<sup>25</sup> extended Wyble's study using net pressures up to 20,000 psi. on four sandstones. The changes in resistivity beyond

5000 psi. are less dramatic than those up to 5000 psi. Redmond presented more data but added little to our understanding of the effects of pressure.

Glumov and Dobrynin<sup>12</sup> reported the effect of pressure on the electrical conductivity of one sandstone and one limestone using net pressures up to 350 atmospheres. The experimental apparatus was similar to Wyble's. One to two hours are typically necessary for equilibrium but Glumov and Dobrynin made their measurements 15-20 minutes after each application of pressure, making it highly unlikely that the cores were measured at an equilibrium condition.

Orlov and Gimeav<sup>20</sup> investigated the changes in resistivity caused by applying all-around stresses of up to 400 atmospheres on two carbonates. The carbonates did not reach equilibrium although a constant pressure was applied for 100 hours. The lower porosity samples were found to be affected to a greater extent than those with higher porosities. At 400 atmospheres the low porosity samples showed increases of 40-80% of the atmospheric resistivity.

Dobrynin<sup>7</sup>, using the same experimental approach as Fatt, investigated the effect of pressure on the resistivity of two sandstones. The observation that compressibility of these sandstones was a function of pressure and that the shale content controlled the number of small pores in a rock which in turn controlled the sensitivity of a rock to overburden pressures resulted in the formulation of a relationship between overburden pressure, porosity, and compressibility

$$\frac{F^P}{F} = \frac{1}{2 \left( \frac{1 - c_p^{\max} F(P)}{1 - \phi c_p^{\max} F(P)} - 1 \right) \phi^{f(P, \frac{c}{c+\phi})}} \quad (1)$$

where  $F^P$  is the formation resistivity factor at any pressure  $P$

$F$  is the formation resistivity factor at atmospheric pressure

$\emptyset$  is the fractional porosity

$C_p^{\max}$  is the pore compressibility at low pressure

$$F(P) = P_{\min} + \frac{P}{\log \frac{P_{\max}}{P_{\min}}} \left( .434 + \log \frac{P_{\max}}{P} - \frac{P_{\min}}{P} \left( \log \frac{P_{\max}}{P_{\min}} + .434 \right) \right) \quad (2)$$

$P_{\min}$  is the pressure at which  $C_p^{\max}$  is obtained

$P_{\max}$  is the extrapolated pressure at  $C_p = 0$

$P$  is pressure

$c$  is the fraction of bulk volume occupied by clay.

Unfortunately this correlation relies primarily on low pressure data which are subject to question in this case because of the Lucite mounting of the core. The Lucite has structural strength and thus will hold some of the applied force off the core. While this is not critical at high pressures it becomes of significance at very low pressures. The porosity exponent  $(f(P, \frac{c}{c+\emptyset}))$  was evaluated as the pressure approached zero and  $C_p^{\max}$  was obtained by straight line extrapolation on coordinate paper to atmospheric pressure. This correlation will be discussed in greater detail later in the paper.

The above-mentioned authors all agreed that the effects of pressure on the resistivity of rocks are appreciable and any interpretation of resistivity measurements not taken at in-situ conditions are subject to errors of from 10 to 120 percent.

In summary it may be said that prior to this work only a modest quantity of data was available on the effects of overburden pressure



on the resistivity of porous rocks and much of this data was of a qualitative nature. Only one investigator attempted to use the data quantitatively and his work used some questionable assumptions. At this time all the effects of pressure must be determined experimentally as there is no reliable technique to predict the effects of pressure on the resistivity of fluid saturated rocks.

Prior to this work no data were available indicating the effect of temperature (with or without pressure) on the electrical resistivity of porous-fluid saturated rocks.

## CHAPTER II

### THEORY

The resistivity (specific resistance) of a material is a physical property like specific gravity, density, or mass. The resistivity of a cube or cylinder is obtained by

$$R = r \left( \frac{A}{L} \right) \quad (3)$$

where: R is the resistivity in ohm-meters

r is the resistance in ohms

L is the sample length in meters, and

A is the cross sectional area of the sample in square meters.

The resistivity of fluid saturated porous media has long been of interest to scientists and engineers. Maxwell<sup>19</sup> theoretically related the resistivity and porosity for a dispersed sphere arrangement by

$$\frac{R_o}{R_w} = \frac{3 - \phi}{2\phi} \quad (4)$$

where:  $R_o$  is the resistivity of the medium 100% saturated

$R_w$  is the resistivity of the saturating fluid, and

$\phi$  is the fractional porosity.

Lord Rayleigh<sup>24</sup> derived a generalized equation for spheres and cylinders of one material dispersed in another in a cubic arrangement.

$$\frac{R_o}{R_w} = 1 + \frac{3P}{\frac{V+2}{V-1} - P - 1.65 \left( \frac{V-1}{V+\frac{4}{3}} \right)^{3.33}} \quad (5)$$

where:  $V = \sigma_2/\sigma_1$ ,  $\sigma_2$  being the conductivity of the spheres and  $\sigma_1$  the conductivity of the liquid

$P = 1-\phi$  where  $\phi$  is the fractional porosity.

For a sandstone model  $V = 0$  ( $\sigma_2 = 0$ ). For large porosities this equation becomes that proposed by Maxwell.

For a nonspherical solid suspended in a liquid Fricke<sup>9</sup> found

$$\frac{\frac{\sigma_x}{\sigma_1} - 1}{\frac{\sigma_x}{\sigma_2} + X} = (1 - \phi) \frac{\frac{\sigma_2}{\sigma_1} - 1}{\frac{\sigma_2}{\sigma_1} + X} \quad (6)$$

where:  $\sigma_2$  is the conductivity of the solid material in suspension,

$\sigma_1$  is the conductivity of the suspension material,

$\sigma_x$  is the conductivity of the suspension, and

$X$  is a shape factor.

For a nonconducting solid the equation becomes

$$\frac{R_o}{R_w} = \frac{X + 1 - \phi}{X\phi} \quad (7)$$

which in turn simplifies to Maxwell's for spheres when  $X$  is 2.

Salwinski<sup>27</sup> formulated the following relationship between porosity and resistivity of a medium with non-conducting spheres in contact in a regular array.

$$\frac{R_o}{R_w} = \frac{(1.3219 - .3219 \phi)^2}{\phi} \quad (8)$$

Dakhnov<sup>6</sup> found that

$$\frac{R_o}{R_w} = \frac{1 + .25 (1 - \phi)^{1/3}}{1 - (1 - \phi)^{2/3}} \quad (9)$$

best represented the relationship between porosity and resistivity for unconsolidated sands.

Pirson<sup>22</sup> calculated the Formation Resistivity Factor for the particular case where the spheres are of equal size. For a cubic packing with a porosity of 47.6% the Formation Resistivity Factor is 2.64. A rhombic packing is anisotropic having a Formation Resistivity Factor of 4.4 in one direction and 3.38 in the other, for a porosity of 39.5%. Hexagonal packing is the closest possible for equal size spheres having a porosity of 25.9% and a Formation Resistivity Factor of 5.81.

One of the few models formulated for consolidated porous media was that build by Owen<sup>21</sup>. The relative size of the pore-to-pore channel connection and the length of the pore channel were variable. The former was termed constriction while the variation of the actual pore length to the shortest possible length was called tortuosity. Holding the constriction factor constant and varying the tortuosity resulted in the shifting of the Formation Resistivity Factor-porosity curve with almost no change in slope as shown in Figure 1. Maintaining the tortuosity constant and varying the constriction factor resulted in a change of slope and the point of intersection at the 100% porosity line. Relating these to a general form of  $F = k \phi^{-m}$ , the tortuosity affects only  $k$  while the constriction changes effect  $m$  and  $k$ . Figure 2 shows the case for constant tortuosity.

Towle<sup>29</sup> derived some particular relationships between porosity

FIGURE 1  
FORMATION RESISTIVITY FACTOR VERSUS POROSITY  
FOR CONSTANT CONSTRICTION FACTOR (C)  
AND VARIOUS TORTUOSITIES (T)

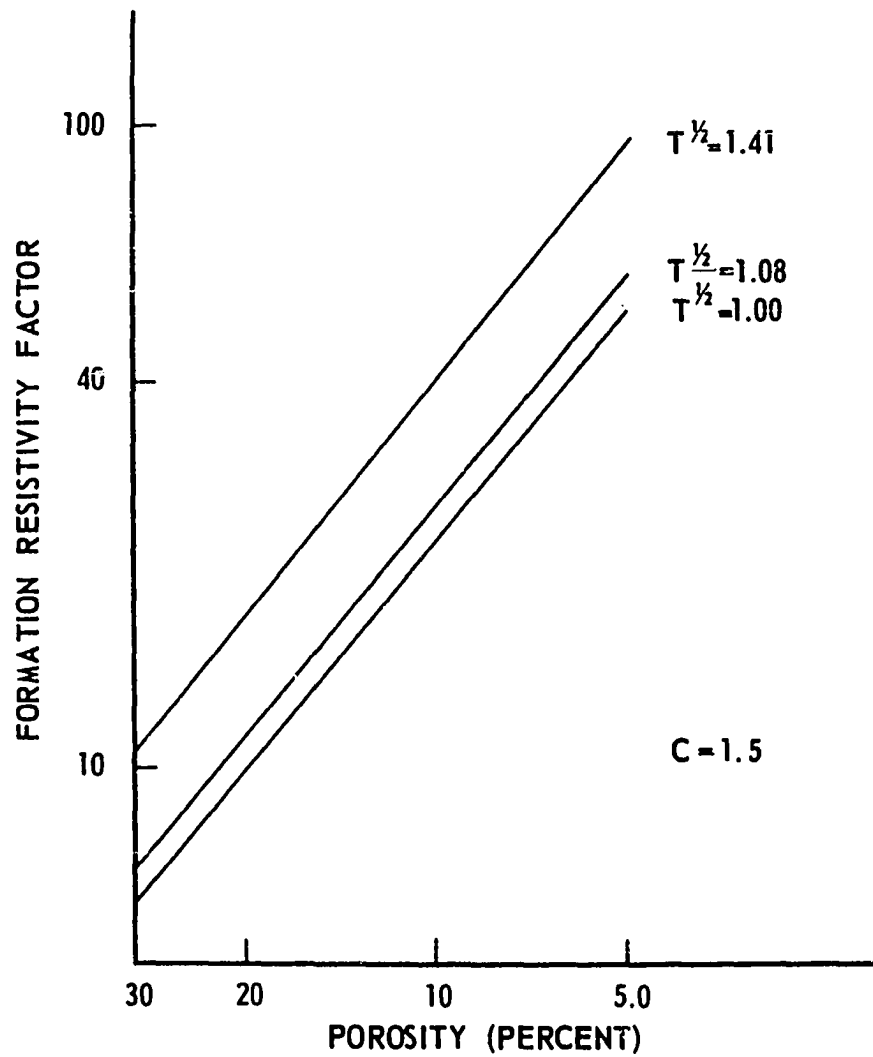
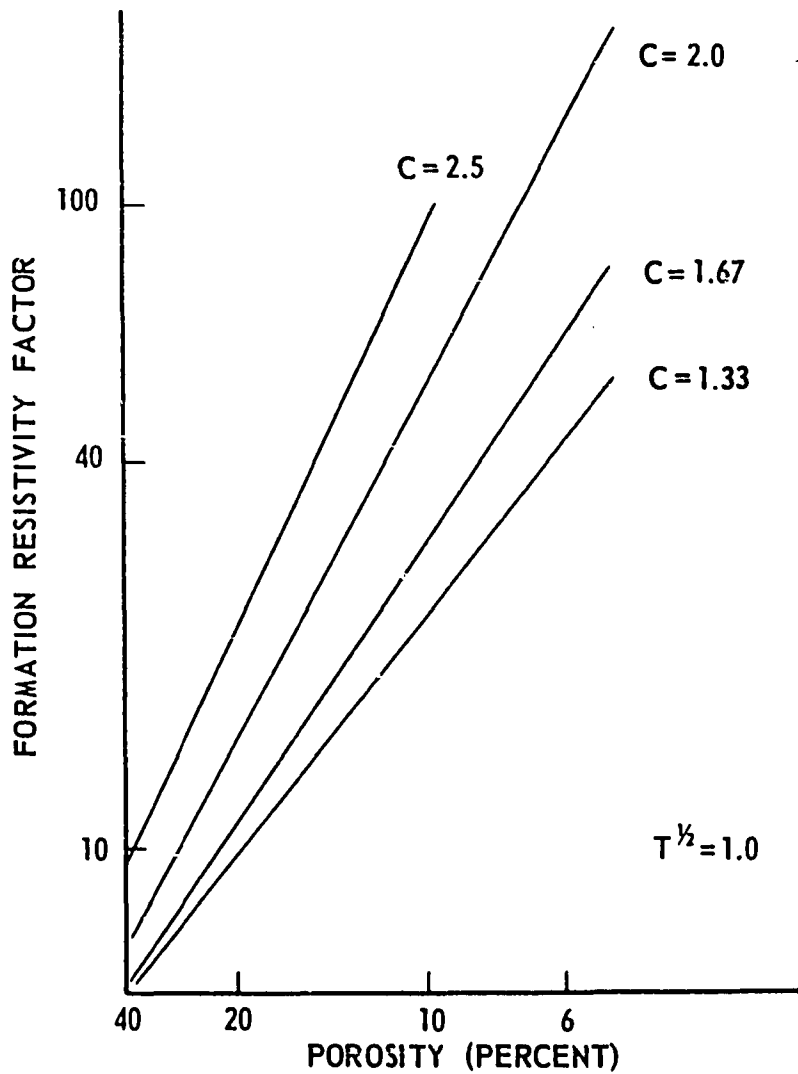


FIGURE 2  
FORMATION RESISTIVITY FACTOR VERSUS POROSITY  
FOR CONSTANT TORTUOSITY (T) AND VARIOUS  
CONSTRICTION FACTORS (C)  
(AFTER OWEN, J. P. T. 1952)



and Formation Resistivity Factor for some idealized consolidated porous media but did not relate them to experimental data and thus they are interesting but of unproven usefulness.

In general the theoretical porosity-resistivity relationships are much too simple to represent the very complex natural rocks. Empirical relationships have therefore become the most important tool in this field. Archie<sup>2</sup> proposed

$$F = \frac{R_o}{R_w} = \phi^{-m} \quad (10)$$

where F is the Formation Resistivity Factor and m is an exponent which varies from 1.3 for unconsolidated media to 2.5 for very consolidated media.

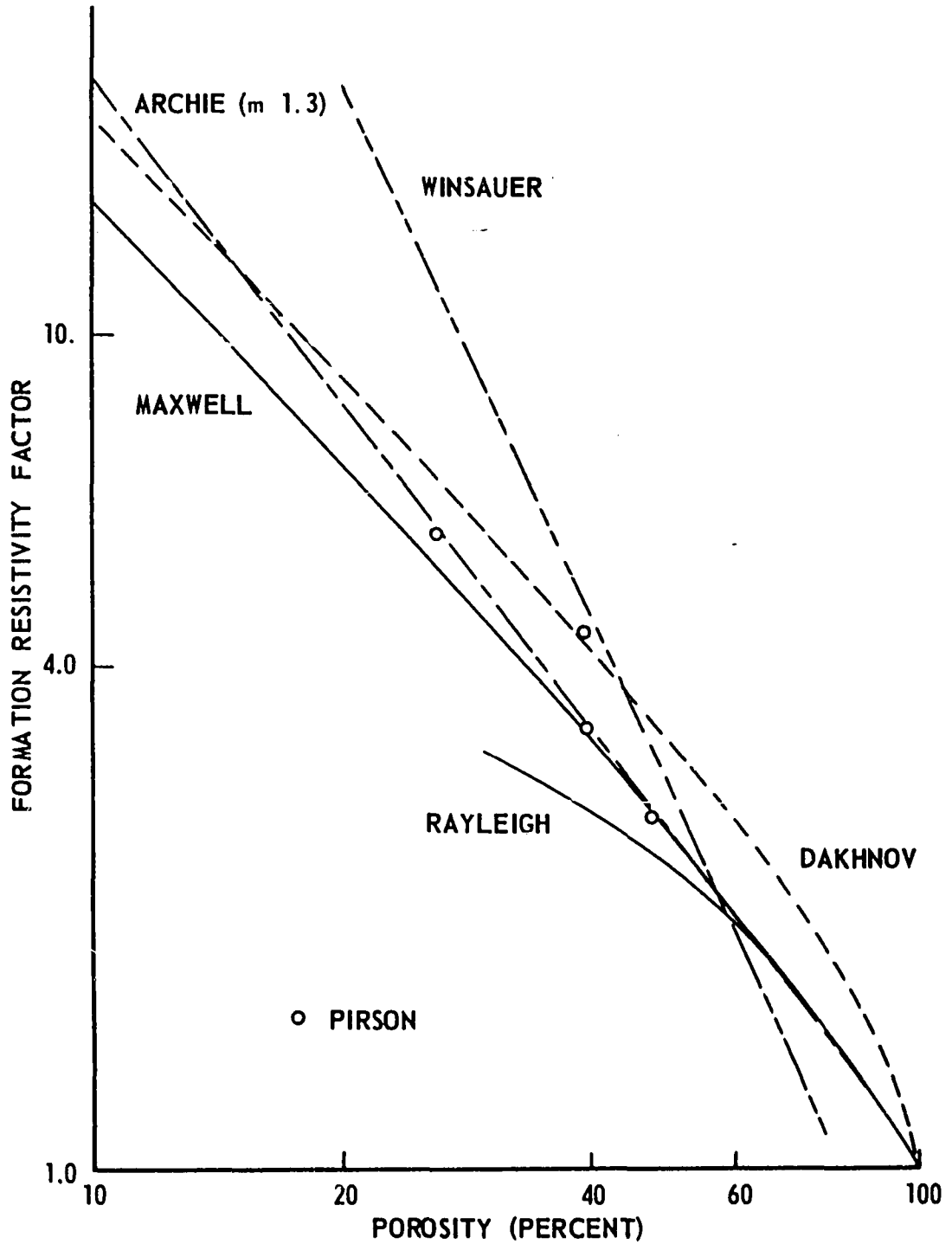
A more general relationship of the same form is

$$F = \frac{R_o}{R_w} = C \phi^{-m'} \quad (11)$$

where C and m' are constants. The most widely used constants for this relationship are .62 and 2.15, respectively, which were determined by Winsauer, et al<sup>30</sup>.

Figure 3 shows a comparison of some of the relationships discussed above. It is obvious that Rayleigh's theory is good only for large porosities. Maxwell and Archie agree fairly well at the higher porosities, while Archie and Dakhnov agree fairly well in the lower porosity range. The Winsauer equation is a specialized effort to obtain a general equation for unconsolidated and consolidated formations over the range of porosities generally encountered in petroleum reservoirs.

**FIGURE 3**  
**COMPARISON OF SELECTED FORMATION RESISTIVITY FACTOR -**  
**POROSITY RELATIONSHIPS FOR UNCONSOLIDATED SANDS**





It appears from the curves that no one relationship will adequately describe the Formation Resistivity Factor-porosity variations in natural rocks. Most of the equations are good over some limited range and for some limited grain shape and sorting. It would appear that the sedimentation process and general geologic history would control the resistivity-porosity relationship. There is a possibility that the geological environment could be determined from a close examination of the resistivity-porosity data for an unconsolidated sand. Some of the many variables which affect the porosity-resistivity relationship are: grain shape, grain sorting, mineral content, cementation, geologic age, geologic history, and homogeneity. A great effort will be needed to understand even a few of the factors that influence the resistivity of porous media.

## CHAPTER III

### PROCEDURE FOR INVESTIGATION

#### FORMATION SAMPLES

The homogeneity of individual samples and over-all variety of composition were stressed in the selection of formation samples. Three sandstones (Berea, Bandera, Briar Hill), one limestone (Paradox), one shale (Dean), and one artificial (Alundum) sample were used. The physical size and porosities of the cylindrical cores are given in Table I. X-ray diffraction pattern analyses were used to determine the composition of the sandstones. The "semiquantitative" results are presented in Table II.

The Alundum was used as a very homogeneous, clay free reference sample, whereas the Berea, Bandera, and Briar Hill samples contained varying amounts of clay. A more detailed description of the samples is available in the Appendix.

#### SAMPLE PREPARATION

The core plugs were squared with a diamond saw and the ends precision ground to insure a smooth flat contact for the end electrodes. The cores were cleaned with toluene, dried, and the porosity measured with a Kobe porosimeter. They were then saturated with 90,000 ppm. aqueous sodium chloride. An aging period of 3-4 weeks was allowed after which the water salinity was checked to determine if contamination

had occurred. Following the experiments the cores were stored in the same brine.

Mercury injection pore size distribution measurements were made on each sample type.

TABLE I  
DIMENSIONS AND POROSITIES OF SAMPLES

Sample	Length (inches)	Diameter (inches)	Pore Volume (cu. in.)	Porosity (%)
Berea A	2.031	1.523	11.219	18.5
Berea 1	2.02	1.492	11.841	20.7
Berea 2	2.01	1.492	11.911	21.0
Berea 3	2.03	1.500	11.696	20.4
Berea 4	2.03	1.492	12.059	20.8
Bandera A	2.031	1.531	13.498	22.3
Bandera B	2.031	1.527	13.069	21.7
Bandera C	2.008	1.523	13.283	22.3
Briar Hill A	2.047	1.523	12.599	21.1
Briar Hill C	2.047	1.523	12.683	21.3
Dean A	2.027	1.527	5.184	8.5
Dean B	2.023	1.531	4.546	7.5
Dean C	2.031	1.527	4.507	7.4
Paradox A	2.016	1.531	.266	.4
Paradox B	2.203	1.527	1.712	2.8
Paradox C	2.023	1.531	.777	1.3
Alundum A	2.+	1.453	14.427	26.4
Alundum B	2.+	1.484	15.090	26.5
Alundum C	2.+	1.453	14.434	26.8

TABLE II

## X-RAY DIFFRACTION ANALYSES OF SANDSTONE SAMPLES

	Bandera	Briar Hill	Berea
Illite	5%	Trace	Trace
Kaolinite and Chlorite	5%	Trace	5%
Quartz	45%	90%	75%
Feldspar	35%	5%	15%
Calcite		Trace	
Dolomite	5%		5%
Siderite	Trace	Trace	Trace

## APPARATUS

### Pressure Equipment

Pressure was exerted on the frame of the rock sample by transformer oil pressing on the elastic sleeve and two stainless steel endplates enclosing the core. The oil was retained by a thick-walled autoclave (3' I.D. x 6') made of C-1018 cold finished steel. The wall thickness was approximately  $1\frac{1}{2}$  inches. The vessel is shown schematically in Figure 5.

Access to the cell was supplied by a removable top to which the core assembly and the electrical connections were attached. Fusite 1/8 (27) NPT-FP electrical connectors were used. All pressure fittings were  $\frac{1}{4}$ -inch standard high pressure fittings adapted to 1/8-inch stainless steel tubing and valves. Photographs of the cell and core assembly are shown in Figures 4 and 6. The complete pressure system was designed to operate at 15,000 psig.

The schematic of the pressure system in Figure 7 shows that the internal (core) and external (overburden) pressure systems were completely separated. The external pressure system was used to apply pressure to the elastic sleeve and thus to the rock frame. The pressure was generated with a 10,000 psi. Blackhawk pump and transmitted to the cell by 1/8-inch tubing. Attached to this main pressure line were a rupture disc rated at 15,000 psi. and two pressure gauges. The 20,000 psi. gauge was always in contact with the main line while the lower pressure 3,000 psi. gauge could be shut off with a valve when the pressures exceeded 3,000 psi. The low pressure gauge was protected by a 3,000 psi. rupture disc. There was also a bladder valve on the

FIGURE 4  
THE HIGH TEMPERATURE AND PRESSURE CELL  
COMPLETELY ASSEMBLED (EXCEPT THERMAL INSULATION)

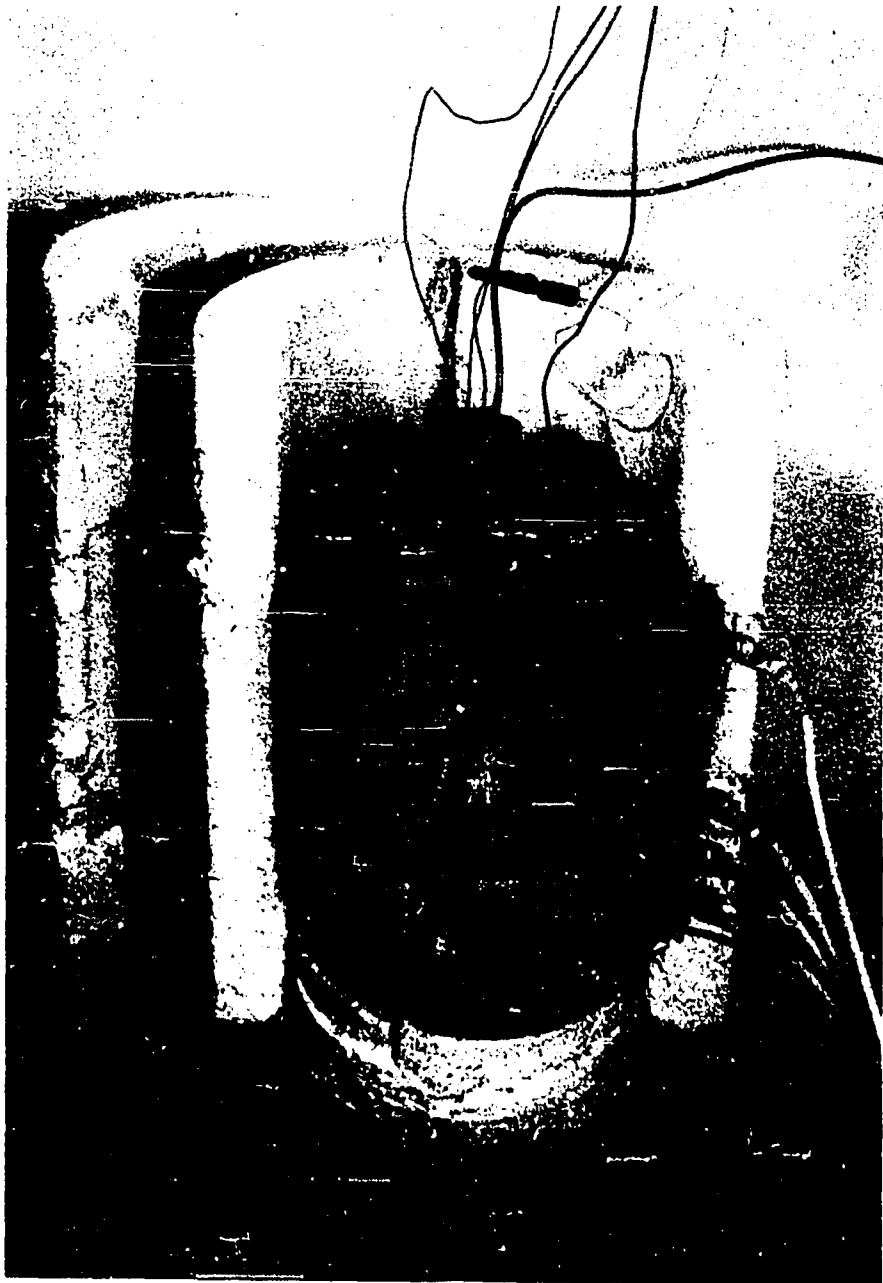


**FIGURE 5**  
**HIGH TEMPERATURE AND PRESSURE RESISTIVITY CELL**

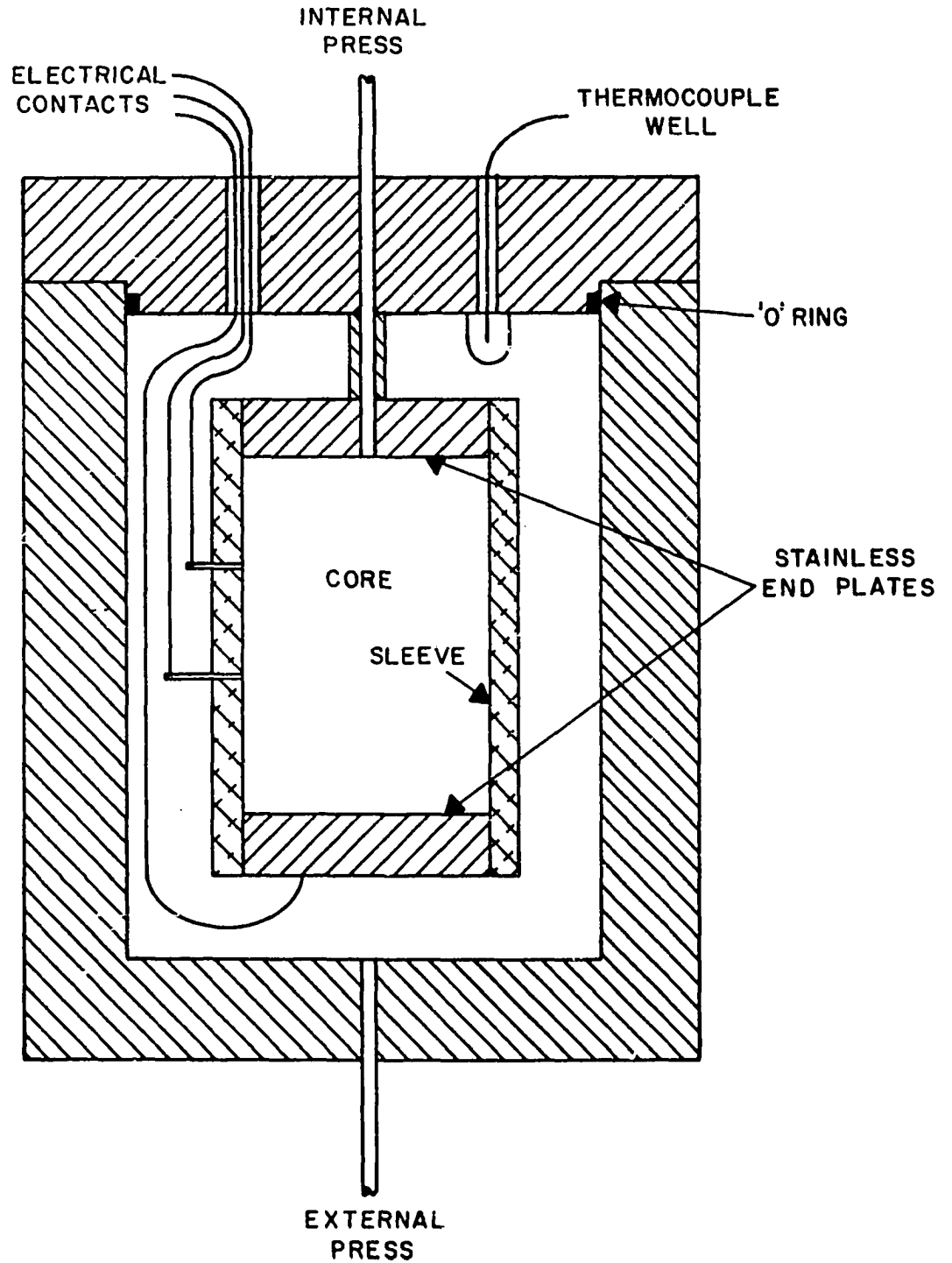
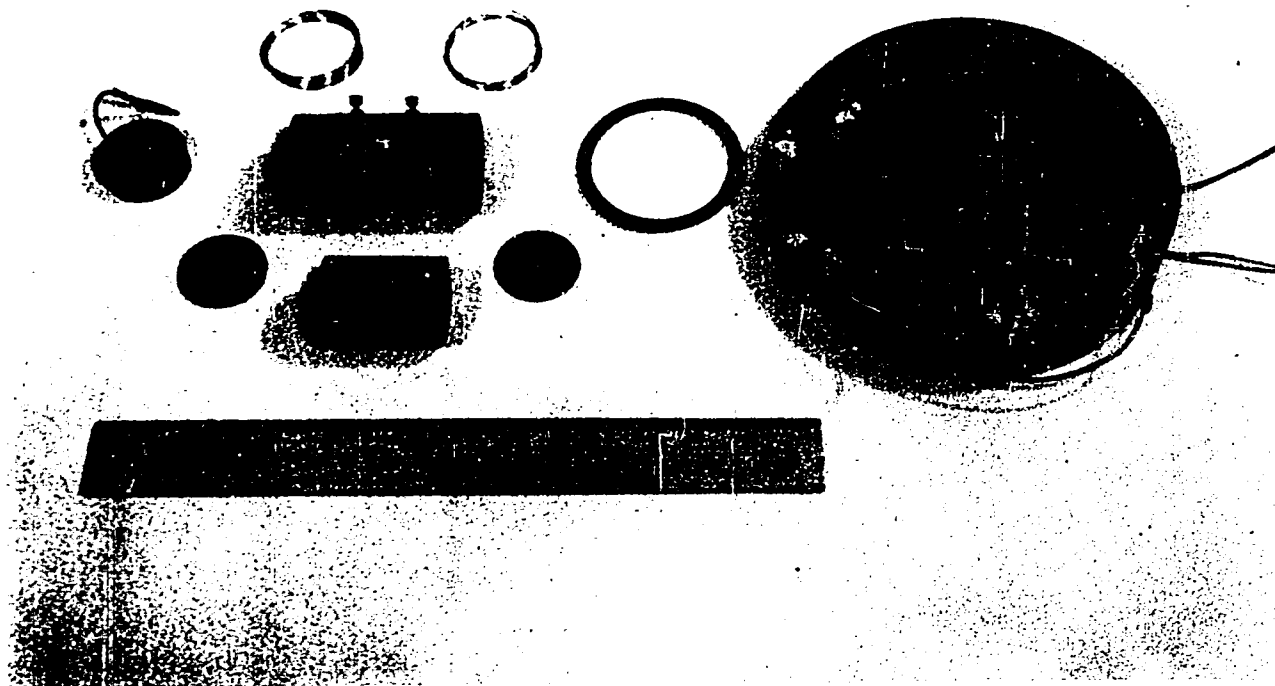
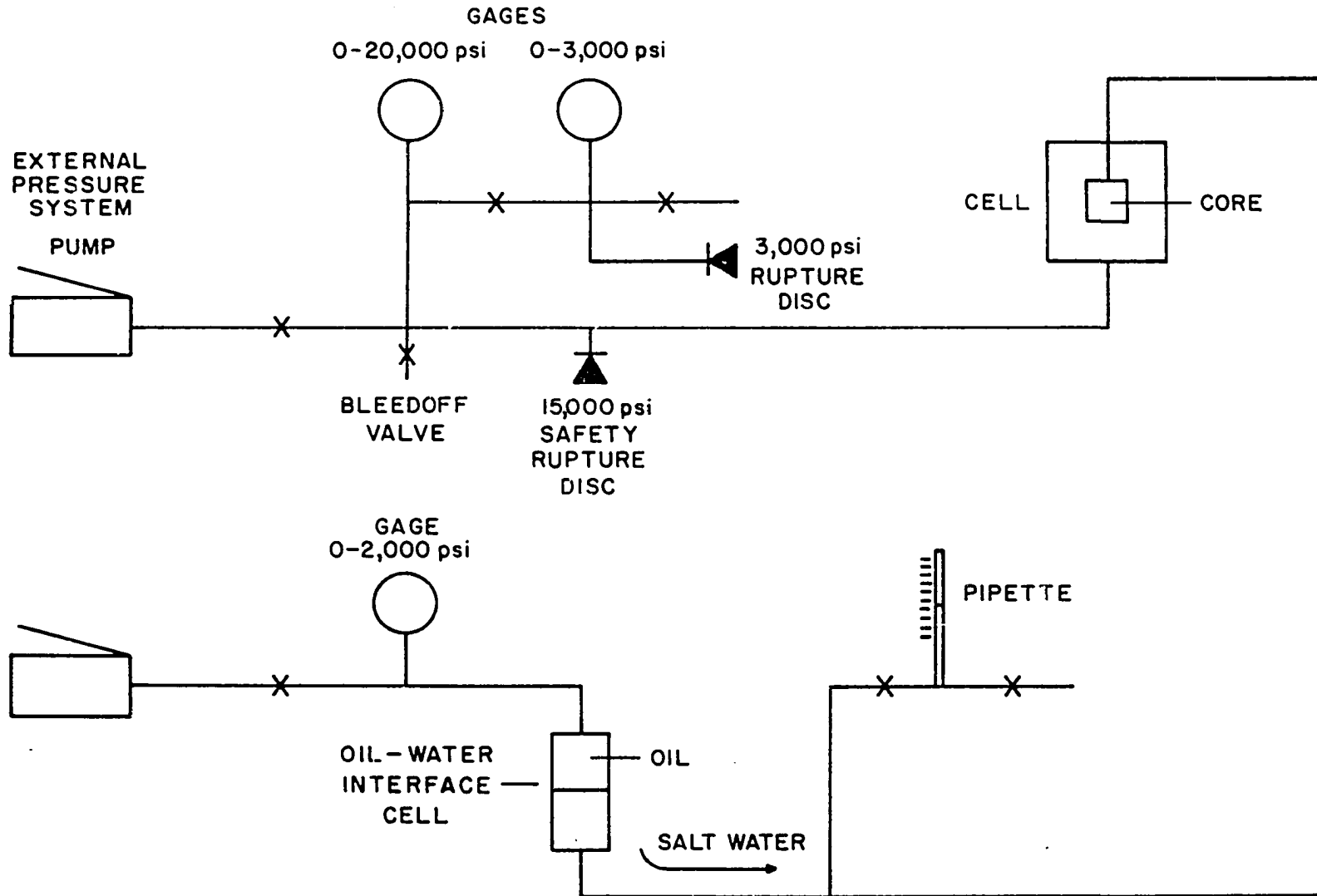




FIGURE 6  
UNASSEMBLED CORE ASSEMBLY AND CELL TOP



**FIGURE 7**  
**SCHEMATIC OF PRESSURE REGULATING SYSTEM**



main line to allow regulation of the pressure system.

The internal or low pressure system which regulated the pressure inside the core used two liquids. The core was saturated with brine while the Blackhawk pump used transformer oil. The two fluids were separated by an interface cell fabricated from a sight gauge. Inside this cell was an indicator or warning system which triggered an alarm when the oil-water interface was in danger of moving into the water part of the system. The warning system consisted of a metal rod which conducted a small amount of current through the water phase in the bottom of the cell. The lowering of the interface to a position where the oil completely covered the rod interrupted the circuit and a buzzer sounded. A schematic of this system is shown in Figure 8.

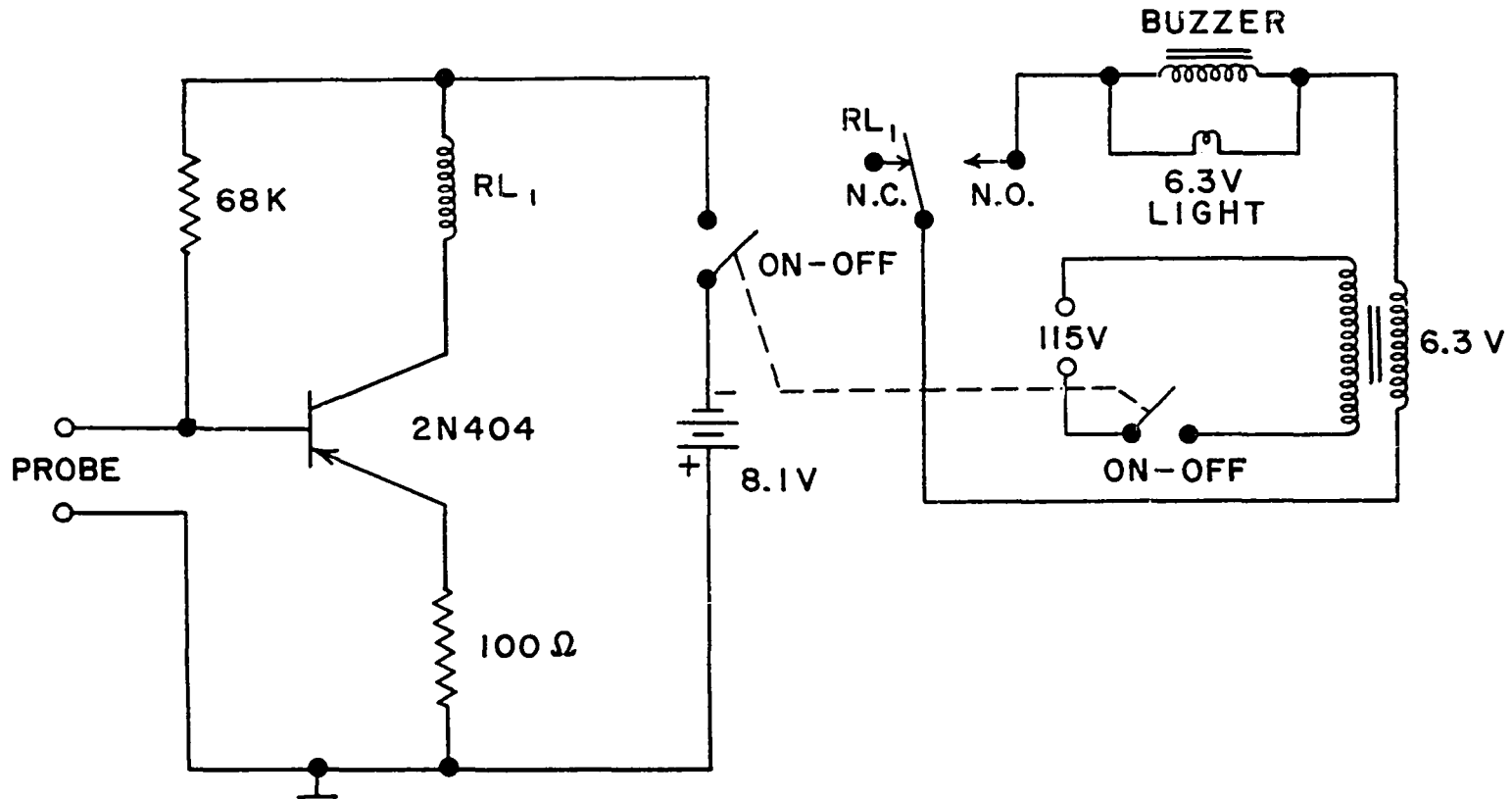
The core was connected to the low pressure system through a hole in the top end plate. The top end plate was in turn attached to the top of the cell with  $\frac{1}{4}$ -inch stainless steel tubing.

The pressure seal for the top was an O-ring made of nitrile rubber (Buna N 382-9). Viton O-rings were tried but they did not contain the pressure at high temperatures. The nitrile O-rings deformed during the first use but could be used numerous times with no leaks or further deformation. They were occasionally replaced as a safety precaution even though no physical defects were encountered.

#### Temperature Equipment

The temperature in the cell was controlled by two electrical heaters cemented to the outside wall of the pressure vessel. The

**FIGURE 8**  
**OIL - WATER WARNING SYSTEM**



$RL_1 = 500 \Omega$ , 9-15 VDC RELAY  
BUZZER OPERATES WHEN INPUT  
RESISTANCE IS  $\sim < 100 \Omega$

2500 watt, 220 volt heater was used for primary control of the temperature while the 500 watt, 110 volt heater was used to maintain the temperature once it was established. The latter was manually controlled with a variable transformer.

The temperature was measured inside the cell with a thermocouple which extended below the top of the cell  $1\frac{1}{2}$  inches. A thermocouple was also placed under the cell to aid in regulating the temperature of the cell. Both thermocouples were calibrated to  $\pm 0.5^\circ\text{F}$ .

### Sleeve Assembly

Neoprene, Hycar, Viton, and silicone rubber sleeves were used during the course of the investigation. The low temperature phase of the experiment was performed with neoprene sleeves. These held up well at low temperatures and could be reused several times. For the low pressure, high temperature phase of the work neoprene was tried but leaked if any difficulty was encountered that lengthened the time necessary to make the experimental run. The neoprene sleeves were replaced by a nitrile rubber (Hycar) which worked very well for this phase of the experiment. Hycar was not tried at high temperatures and pressures because of its low temperature rating.

The high pressure and temperature experiments were started with Viton (fluorocarbon rubber) sleeves. The temperature rating for Viton was sufficiently high but the Viton deformed badly and could be used only once. A reddish colored dye was expelled from the Viton at high temperatures and it impregnated the cores. Tests indicated that no appreciable change in brine resistivity took place upon the addition of this dye. The Viton sleeves were replaced by

silicone (LS 63) rubber sleeves. The silicone rubber deformed slightly, had no noticeable bad effects, and could be used 3 or 4 times before it was replaced.

Trouble was encountered early in the experiment due to the leaking of the sleeves at the core-end plate junction. This was solved by placing a piece of  $3/64$ -inch thick, lead foil between the core and the end plate. This soft metal deformed to fit the core and filled up the voids between the core and the end plate preventing the extrusion of the rubber into these small holes. The lead worked satisfactorily except during the high temperature and pressure experiments. High temperature and pressure caused the lead to flow into and plug the internal pressure regulating hole in the upper end plate. The lead was replaced by cadmium for the high temperature and pressure experiments. Cadmium was less malleable than lead but soft enough to create a good seal and make a good electrical contact with the core.

The resistivity measuring system used in this work necessitated the placing of two potential measuring electrodes along the side of the core. These electrodes were small ( $2/56$ ) stainless steel nuts and bolts placed through the side of the sleeve. The head of each bolt was filled with silver solder and then ground flat to approximately the original head thickness. Filling the screw driver slots in the bolt heads prevented the extrusion of the sleeve elastomer between the bolt head and the core. The sleeve was then placed on a mandril and 2 - #50 holes were drilled through the side, one inch apart, parallel to the axis of the sleeve. The bolts were then pushed

through the holes from the inside so that the heads would contact the core when it was placed in the sleeve. A washer was placed on the extending end of the bolt followed by a nut. The nut was tightened until the head of the bolt appeared to be parallel with the inner surface of the sleeve. If the nut was too tight the sleeve would create a bump on the sleeve and the electrode would not contact the side of the core. Once the core was placed in the sleeve the continuity was checked between the potential electrodes and the end plates. If the potential electrodes did not make good contact with the core, the nut was loosened until it was satisfactory. Once the potential electrodes were in a sleeve they were left in place until the sleeve was discarded. The changing of potential electrodes generally resulted in leaks in the sleeve around the bolts.

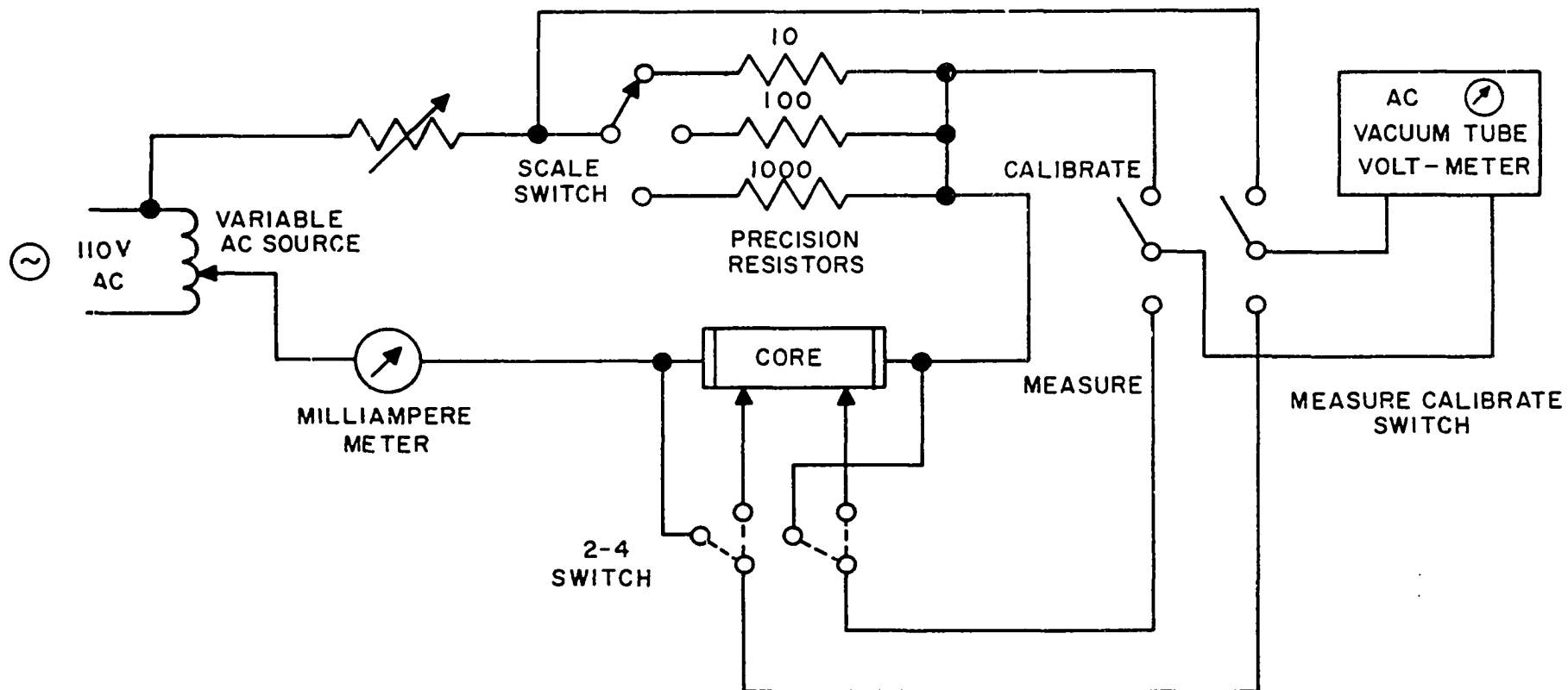
#### Porosity Change Apparatus

The changes in the core porosity were measured with a calibrated pipette which had a total volume of 0.2 ml. and could be read to 0.0002 ml. The pipette was attached to the core by 1/8-inch stainless steel tubing and a hole through the upper electrode assembly of the cell. A light was directed on the pipette so that the water-air interface could be seen easily.

#### Resistivity Measuring Apparatus

The convertible two to four electrode resistivity measuring device used to measure the resistivity of the cores is shown schematically in Figure 9. This system is similar to that of Rust<sup>26</sup>. A four-electrode system has two electrodes in contact with the ends of the core which carry the current and two electrodes along some

**FIGURE 9**  
**SCHEMATIC OF RESISTIVITY MEASURING SYSTEM**





portion of the side of the core which measure the potential drop. A two-electrode system does not have special potential electrodes but measures the potential between the end electrodes. Two-electrode systems are very sensitive to any distortions of current density at the core-electrode contacts and in many cases must be calibrated for the full range of resistivities to be measured. A four-electrode system is not sensitive to contact resistances at the current electrodes because the potential electrodes are generally far enough away from the ends of the core to allow the current density to become uniform.

A variable voltage 60-cycle current was passed through the core, a precision resistor, and a milliammeter all of which were in series. A vacuum tube voltmeter (VTVM) was placed across the precision resistor and the voltage adjusted until the meter read full scale. The VTVM was then placed across the core to make certain the current remained constant. The resistance was then obtained by the following theory:

on calibrate  $I_c = \frac{V_c}{r_c}$

on measure  $I_m = \frac{V_m}{r_m}$

as  $I_c = I_m$

then  $\frac{V_c}{r_c} = \frac{V_m}{r_m}$

and  $r_m = \frac{V_m}{V_c} r_c = (\% \text{ deflection}) \times r_c$

The resistance of the unknown was thus obtained as the percentage deflection of the VTVM times the calibration resistor value. The voltage measuring instrument (VTVM in this case) had to be linear. The accuracy of the measurement was the accuracy of the calibration resistor. Changes in lead resistance from one measurement to another did not affect the readings as a calibration was performed for each measurement. This was essential as the leads in and around the cell changed temperature with the cell and thus changed resistance. The VTVM used was a 10-cycle per second battery-operated Hewlett Packard 404A. The difference between the measuring frequency and the VTVM frequency reduced the noise level of the measurements. The internal resistance of the VTVM was 0.5 megohms and thus the current required by the voltage measuring system was very low and for all practical purposes did not disturb the current flow through the core.

#### EXPERIMENTAL PROCEDURE

The experiment was separated into three phases. The resistivity of the samples was measured at various pressures holding the temperature constant, at various temperatures at constant pressure, and finally at varying temperatures and pressures applied simultaneously. The temperature and pressure in the latter phase needed to be increased at the same rate for each experiment and thus some pressure-temperature relationship was necessary. The point of 100°F. and 1000 psig. was considered a good initial point to correlate with the temperature data and a maximum external pressure of 10,200 psig. was chosen to allow a net stress on the rock of 9000 psi. at 400°F. It was not deemed

advisable to exceed 10,000 psig. and 400°F. to any extent because of the sleeve and O-ring problems being experienced at the time the decision was made. These end point conditions and the use of a linear pressure-temperature relationship resulted in using

$$P = \frac{80}{3} T - 1664 \quad (12)$$

where: P is the net stress in psi. and,

T is the temperature in °F.

The actual external pressure was 1200 psig. above the net stress as the internal pressure was 1200 psig.

The core to be mounted in the elastic sleeve was placed in a beaker of brine. The sleeve was slipped over the core while still submerged, to a position where the end of the core and the sleeve were flush. The solid lead foil disc was placed against the recessed end of the core, followed by the end plate. The top part of the pressure vessel was placed upside down with the attached top end plate facing up. The duct in the end plate and cell top was filled with brine. The lead disc with the 3/32-inch hole in the center was placed on the top end plate. The flush end of the core and sleeve were placed on the top end plate and the sleeve slid over the assembly until the sleeve completely covered both end plates. Number 22 wire was then wound tightly around the sleeve forcing it against the sides of the end plate. The wire was soldered at two places after five or six winds were in place. The ends of the wire were then twisted together to make sure the wire would not come off.

The electrical leads from the top of the cell were connected

and the continuity checked as previously described.

The core assembly was then placed in the cell and the head bolted down. The cell was filled with oil and all electrical and pressure connections attached. A slight pressure was placed on the sleeve and released to expel any water between the core and the sleeve.

The procedure from this point on varied with the phase of the experiment being performed. During the first phase the pressure was usually raised to 300, 900, 1500, 2500, 3500, 4500, 6000, 8000, and 10,000 psig. The pressure at each level was maintained until the resistivity of the core and the pore volume were constant. The resistivity of the sandstones reached equilibrium in 30 minutes to one hour and the pore volume reached equilibrium in one to two hours. Resistivity and pore volume measurements were made every 15 to 20 minutes.

The variable temperature and constant net stress experimental runs required the core to be initially stressed. An internal pressure of 1100 psig. was applied to prevent boiling of the brine at 400°F. At the same time a 2100 psig. external stress was applied to give a net stress of 1000 psi. This net stress was maintained throughout the experimental run.

Initially, equilibrium was attained at a net stress of 1000 psi. following which the temperature was raised in increments of approximately 50°F. The temperature was manually regulated and thus a large amount of experience factor was applied in obtaining constant or near constant intervals in readings. To raise the temperature both heaters were turned on. The temperature at the outside surface

of the vessel was observed and when the external temperature was within 35°F. of the desired temperature both heaters were turned off. The internal temperature then "coasted" to the desired temperature. The desired temperature was held by turning on the 500 watt heater and adjusting the variac so that a small temperature difference was maintained between the inside and outside of the cell. Inasmuch as an increase in the temperature of the vessel caused the fluid to expand and increase the pressure, liquids were bled off both the internal and external systems to maintain a constant pressure. The existence of a constant resistivity and a constant pore volume was assumed to constitute equilibrium. This generally occurred 1 to 1½ hours after the cell reached the desired temperature.

During the third phase, the temperature and pressure were raised simultaneously using the same procedure as the second phase except that the external pressure was allowed to rise to the desired level before bleeding off oil.

The changes in porosity were only determined for the variable pressure experiments. Some data was collected during the elevated temperature and pressure cases but the corrections necessary to adjust the data for the variation in temperature were very large because of the size of the system, which was dictated by safety considerations. Expansion data for aqueous sodium chloride were available up to 200°F. beyond which it was necessary to extrapolate using the assumption that the expansion of the brine was the same as that of pure water. The latter was not acceptable because the two sets of data began to deviate around 200°F. The variation in this

assumed function could easily be larger than the very small so-called porosity changes calculated. It was thus decided that until adequate data on aqueous sodium chloride expansions due to temperature were available these corrections were meaningless.

## CHAPTER IV

### DISCUSSION OF THE DATA ACCURACY

#### PRESSURE

The pressure in the autoclave was measured with two gauges. Pressures up to 3000 psig. were measured on an Ashcroft gauge while the pressures between 3000 and 10,000 were measured on a 20,000 psig. Marsh gauge. These gauges could be read to  $\pm 5$  psig. and  $\pm 25$  psig., respectively. Both gauges were dead weight tested and calibrated. The accuracy of the Ashcroft gauge was 0.2% at full scale and 0.5% at 1000 psig. The accuracy of the Marsh gauge was 0.25% at 10,000 psig. and 1% at 3000 psig. The pressure measurements are considered to be within 1%.

During one Briar Hill experiment the Viton sleeve intruded into the core. The Viton deformed badly under high pressure and temperature. The Briar Hill pores were relatively large and the core was penetrated 3 to 4 grain diameters. This was the only case in which the sleeve was observed penetrating a core. Generally, the sandstone cores allowed the lead foil discs to penetrate the ends up to one grain diameter under high pressure and/or temperatures. This was possibly the reason the two electrode resistivity measurements were erratic and could not be used. The resistivity measurements used were not affected because they were made over the center portion of the core between the two potential electrodes.

The pressure applied to the core was assumed to be uniform throughout the core.

### RESISTIVITY

The resistivity measuring system according to theory, and in fact, measured the resistivity within  $\pm 1\%$ . The resistivity system was checked for accuracy using precision resistors covering the complete range of readings made.



## CHAPTER V

### RESULTS AND ANALYSIS OF DATA

#### PRESSURE EXPERIMENTS

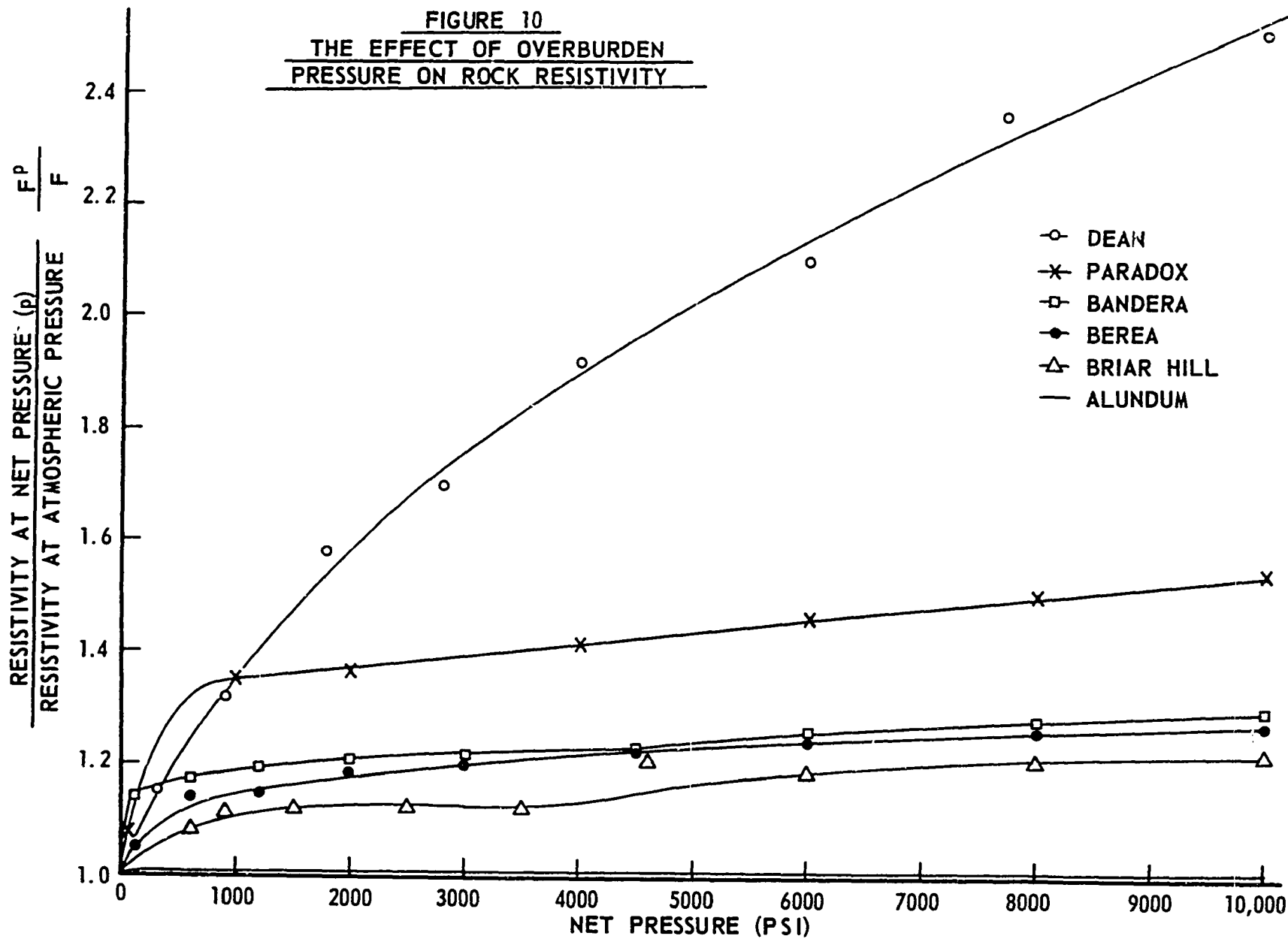
The application of simulated overburden pressure resulted in an increase in the resistivity of the rocks. The resistivity increased rapidly with stresses up to 1000 psig. after which the rate of increase continually lessened as increased stresses were applied with the exception of the Paradox limestone which reached a constant rate of increase above 1000 psig. The effects of net pressure on the relative Formation Resistivity Factor (the Formation Resistivity Factor at pressure  $p$  divided by the Formation Resistivity Factor at atmospheric pressure) of the Alundum, Bandera, Berea, Briar Hill, Dean, and Paradox are portrayed in Figure 10.

Figure 11 is a comparison of data of Fatt, Redmond, Glanville, and the author. The data all have the same general shape although the data of Redmond and the author increase more rapidly up to 1500 psi. This is possibly due to the more flexible core mountings used. Glanville's sample was a limestone and thus not directly comparable. The porosities of the compared samples are approximately the same.

Mercury injection pore size distribution measurements were made on all sample types and are shown in Figures 12 to 17.

The correlation of the relative Formation Resistivity Factor with net stress is a problem with many facets. It appears possible

FIGURE 10  
THE EFFECT OF OVERBURDEN  
PRESSURE ON ROCK RESISTIVITY



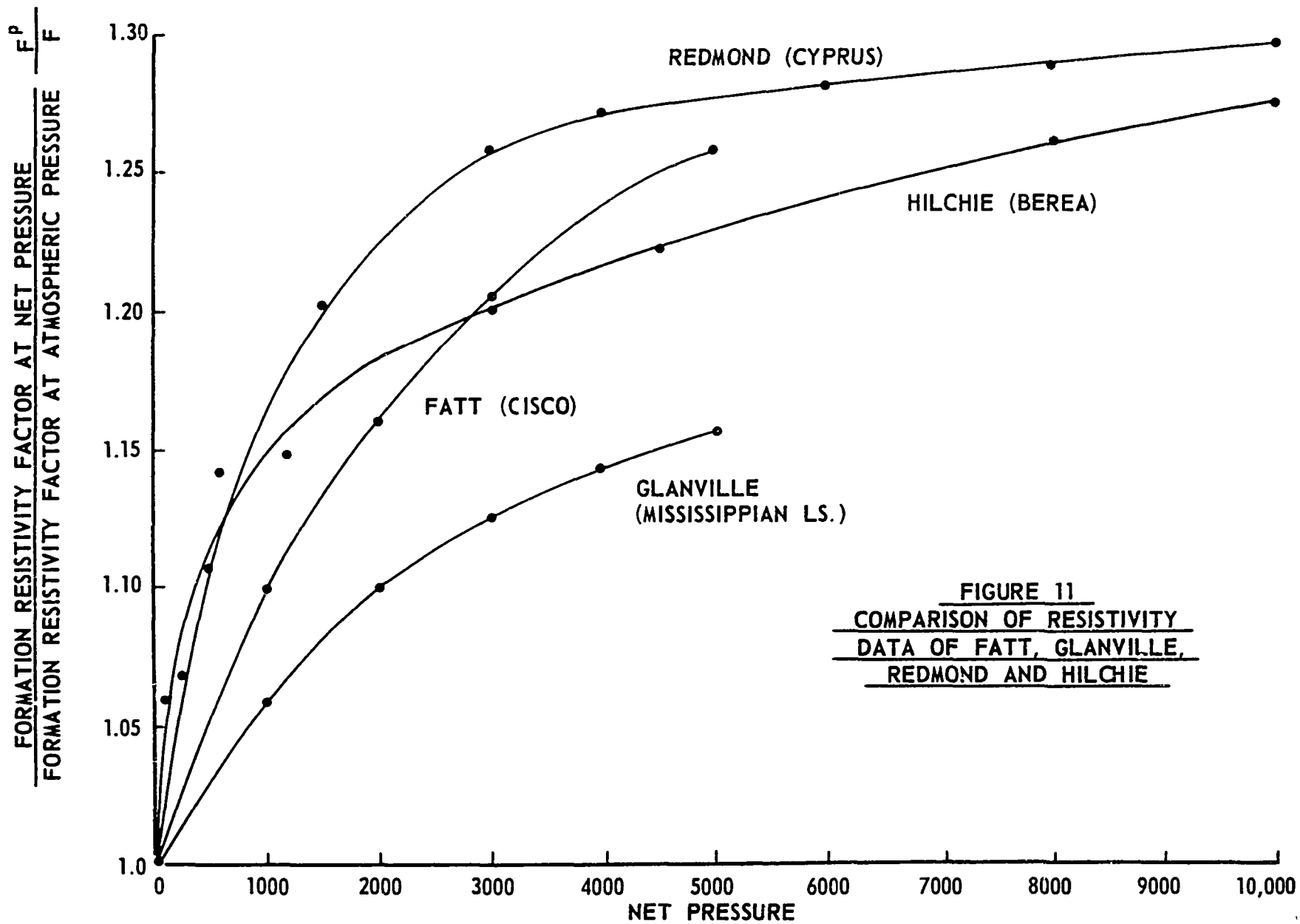


FIGURE 11  
COMPARISON OF RESISTIVITY  
DATA OF FATT, GLANVILLE,  
REDMOND AND HILCHIE

FIGURE 12  
MERCURY INJECTION  
PORE SIZE DISTRIBUTION  
FOR ALUNDUM  
(POROSITY 26.5%)

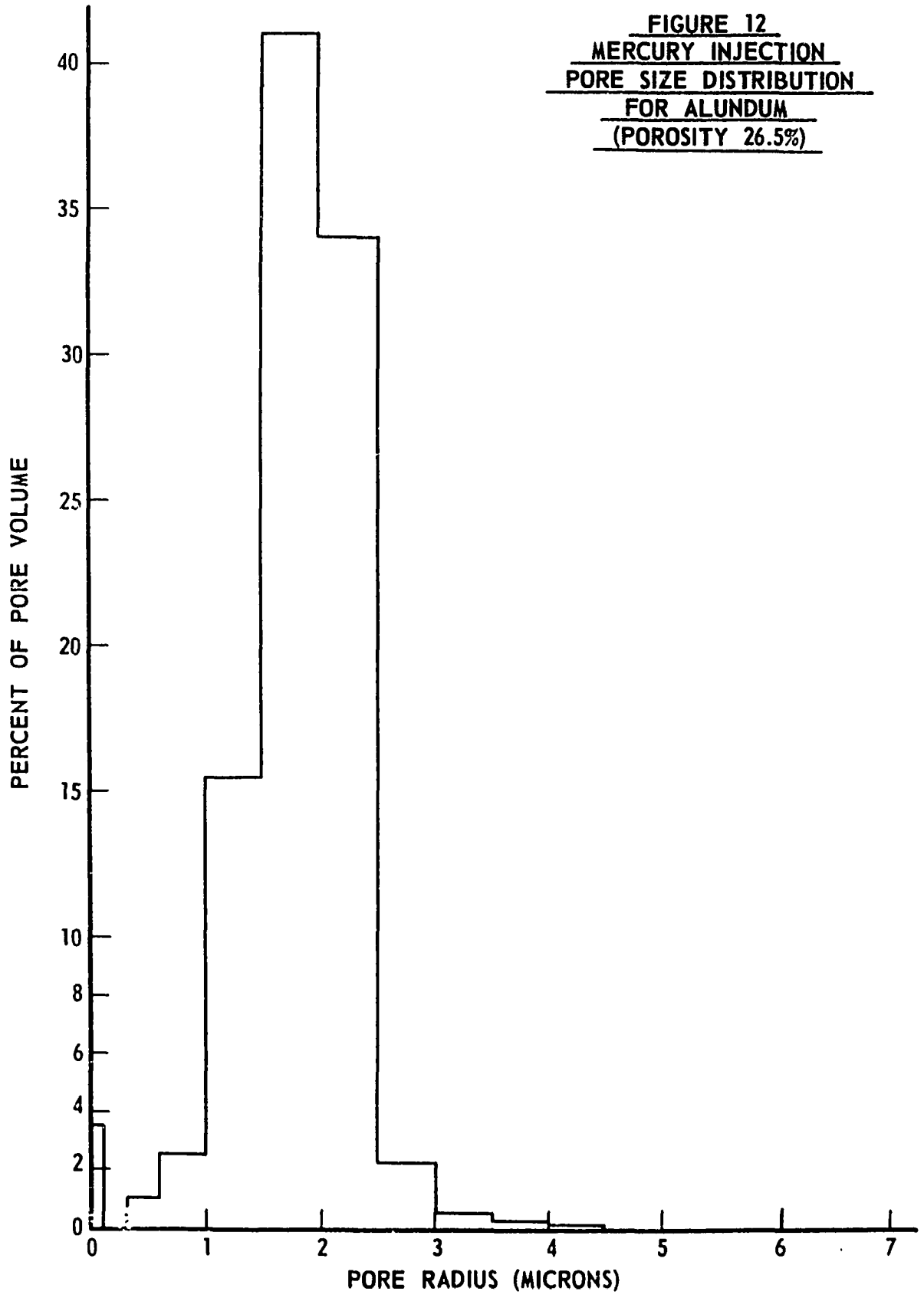


FIGURE 13  
MERCURY INJECTION PORE SIZE  
DISTRIBUTION FOR BANDERA  
(POROSITY 22.7%)

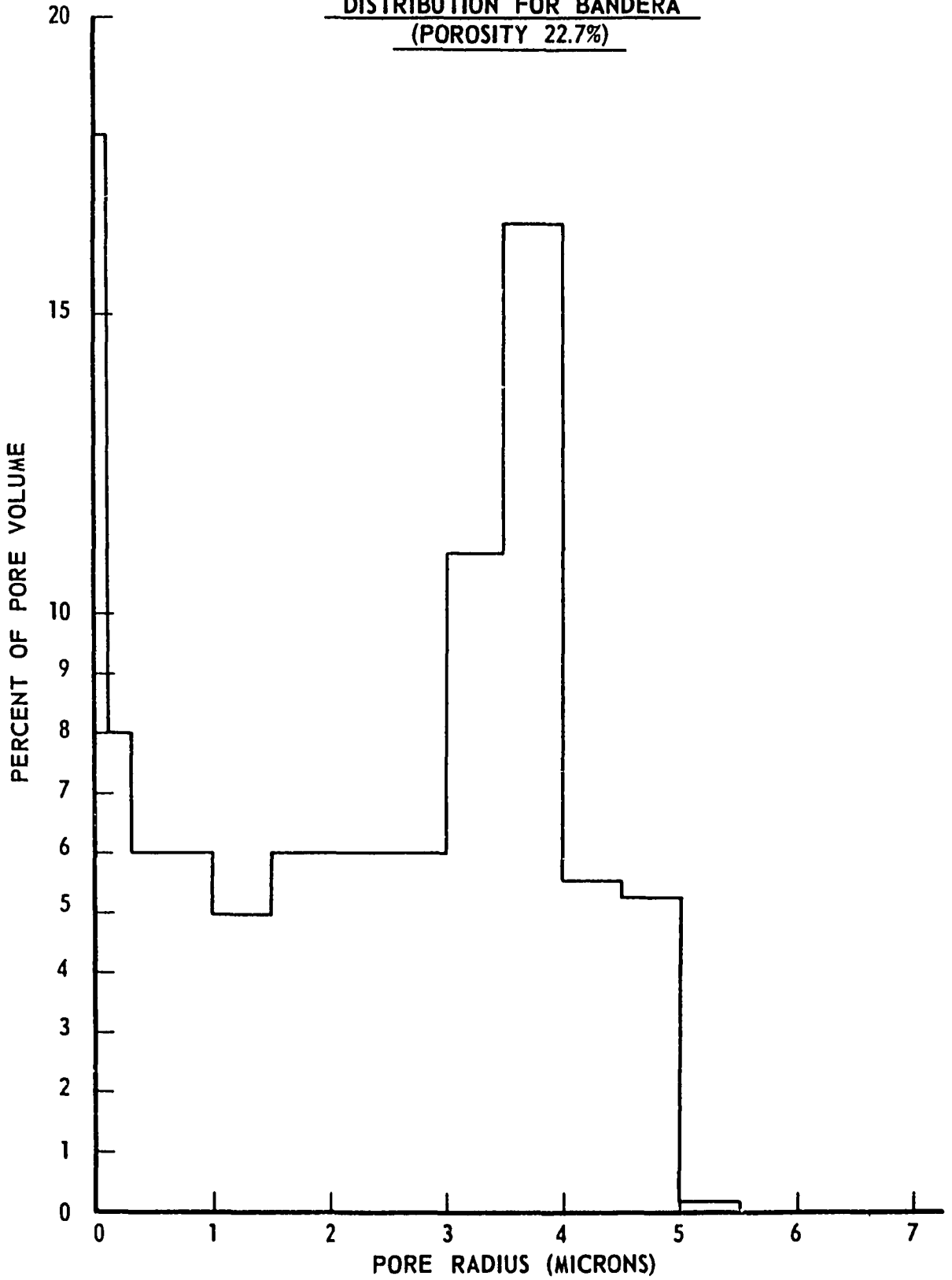


FIGURE 14  
MERCURY INJECTION PORE SIZE  
DISTRIBUTION FOR BEREA  
(POROSITY 20.8%)

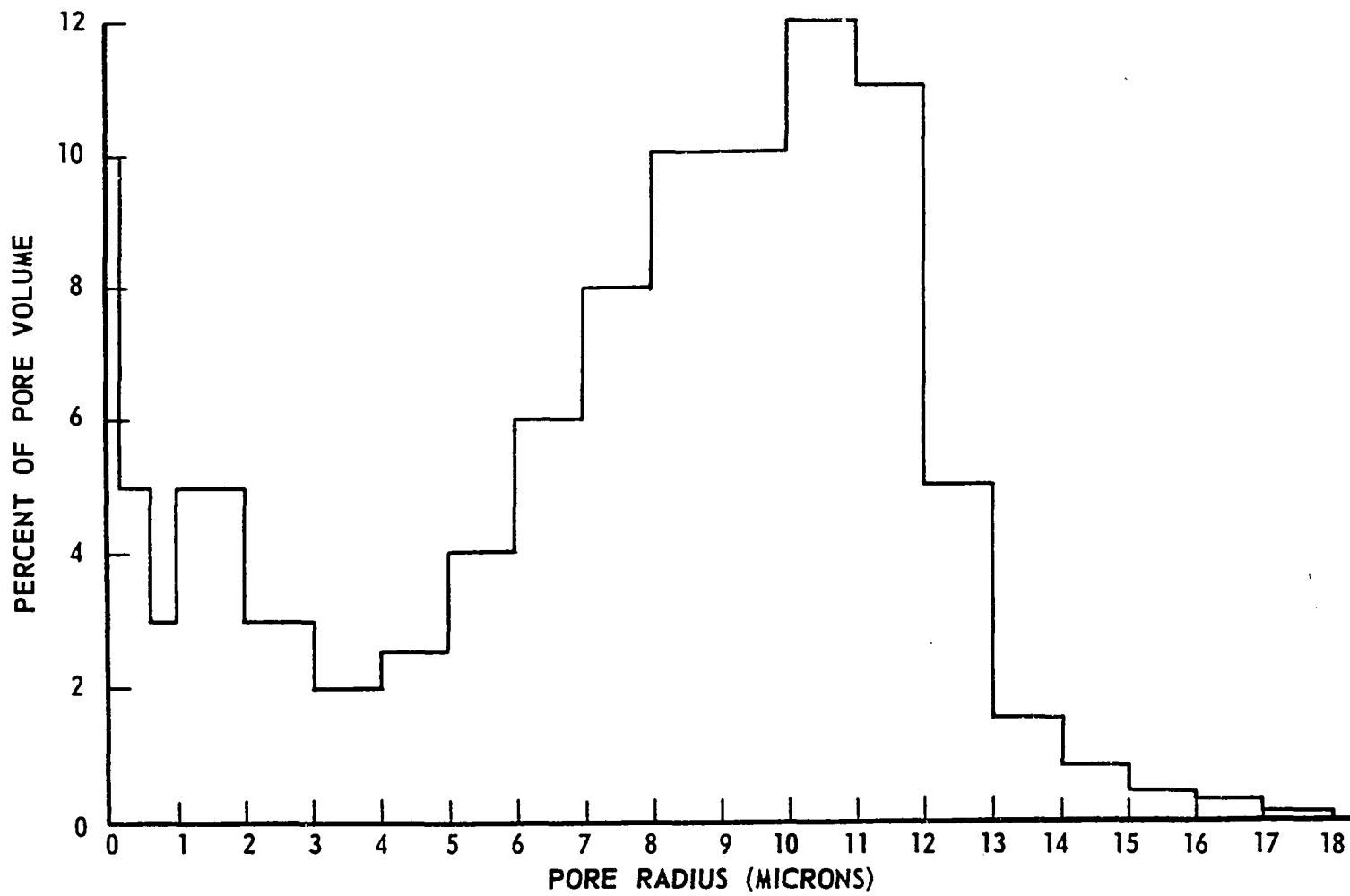


FIGURE 15  
MERCURY INJECTION PORE SIZE  
DISTRIBUTION FOR BRIAR HILL  
(POROSITY 22.0%)

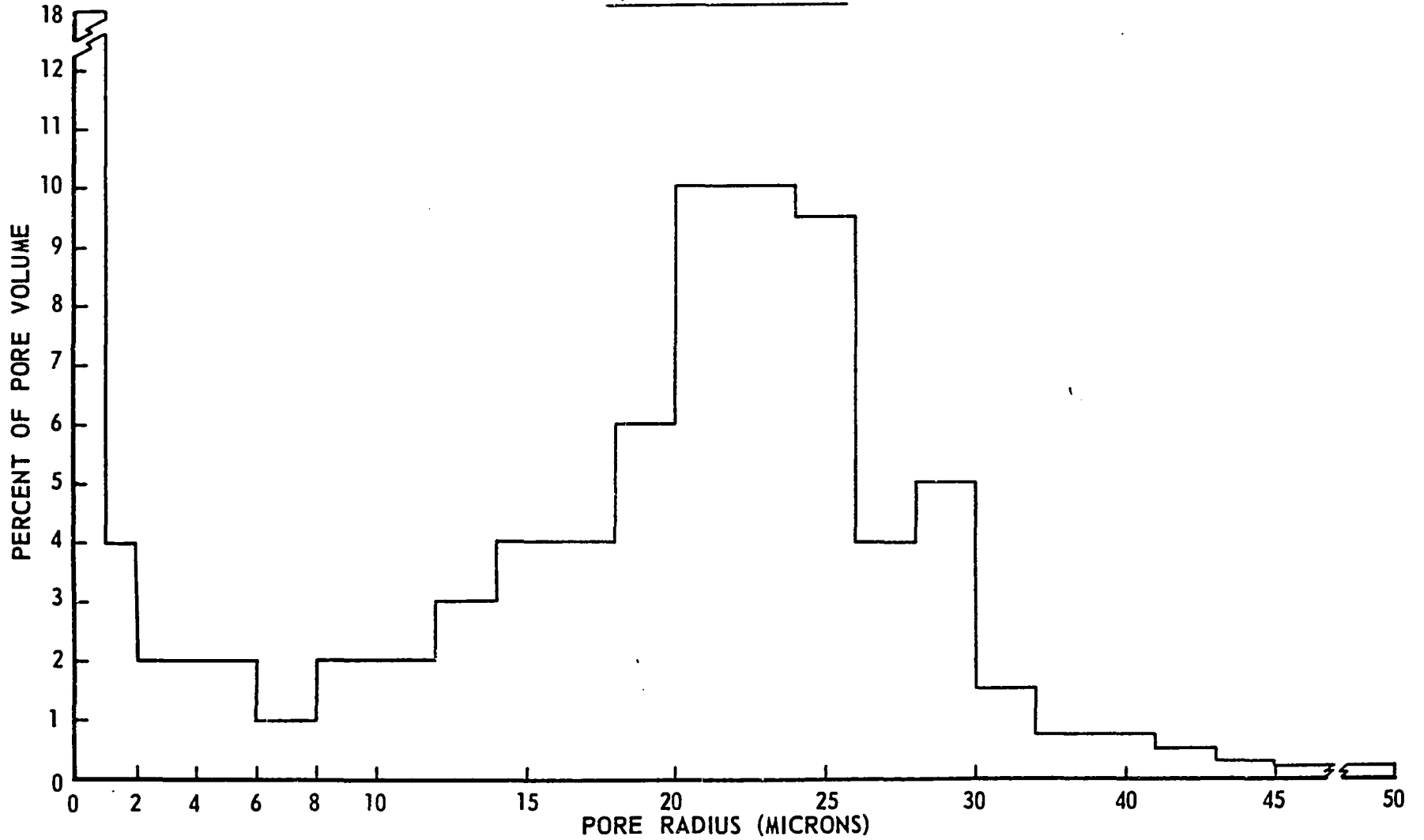


FIGURE 16  
MERCURY INJECTION PORE SIZE  
DISTRIBUTION FOR DEAN  
(POROSITY 9.1%)

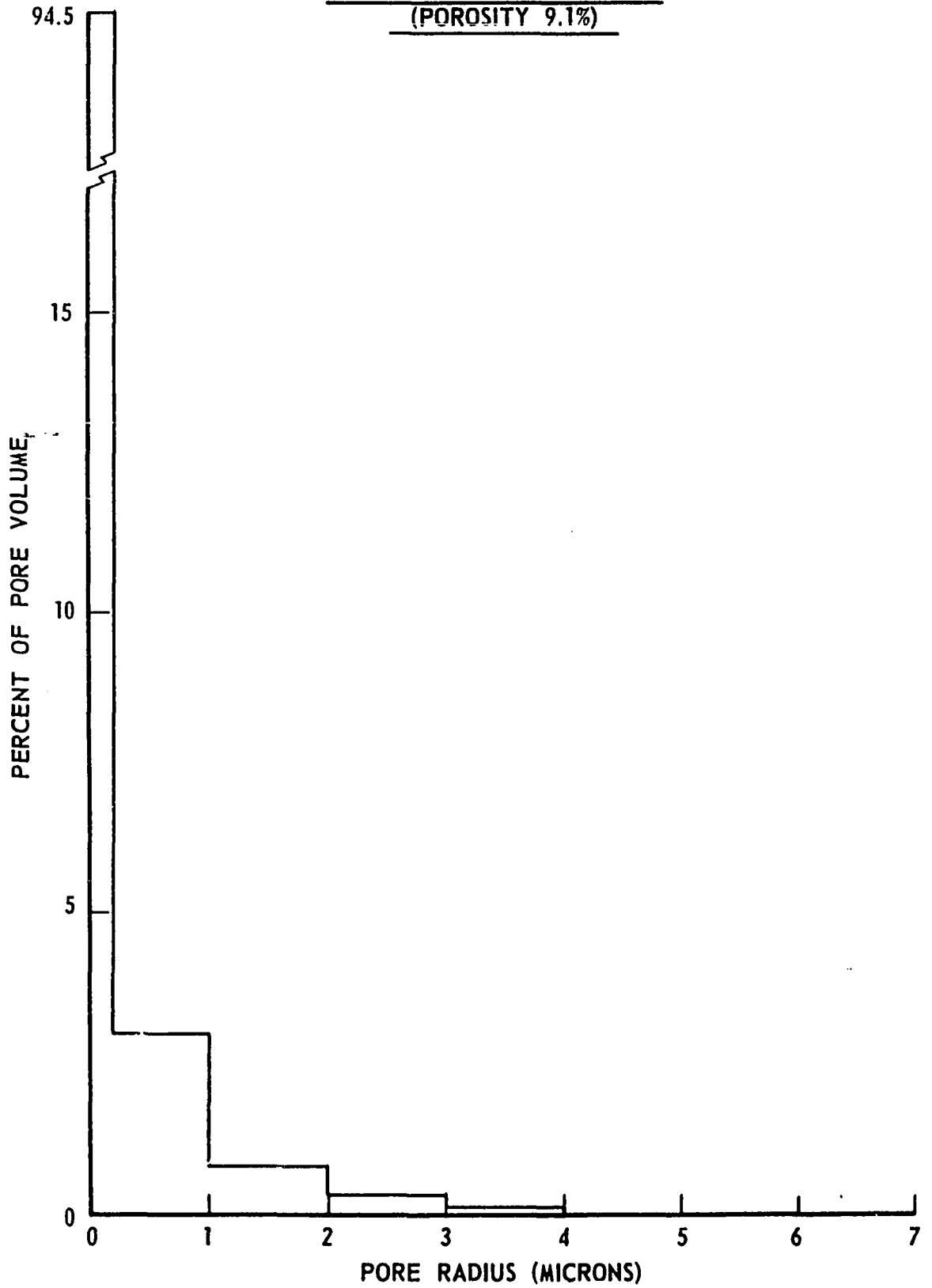
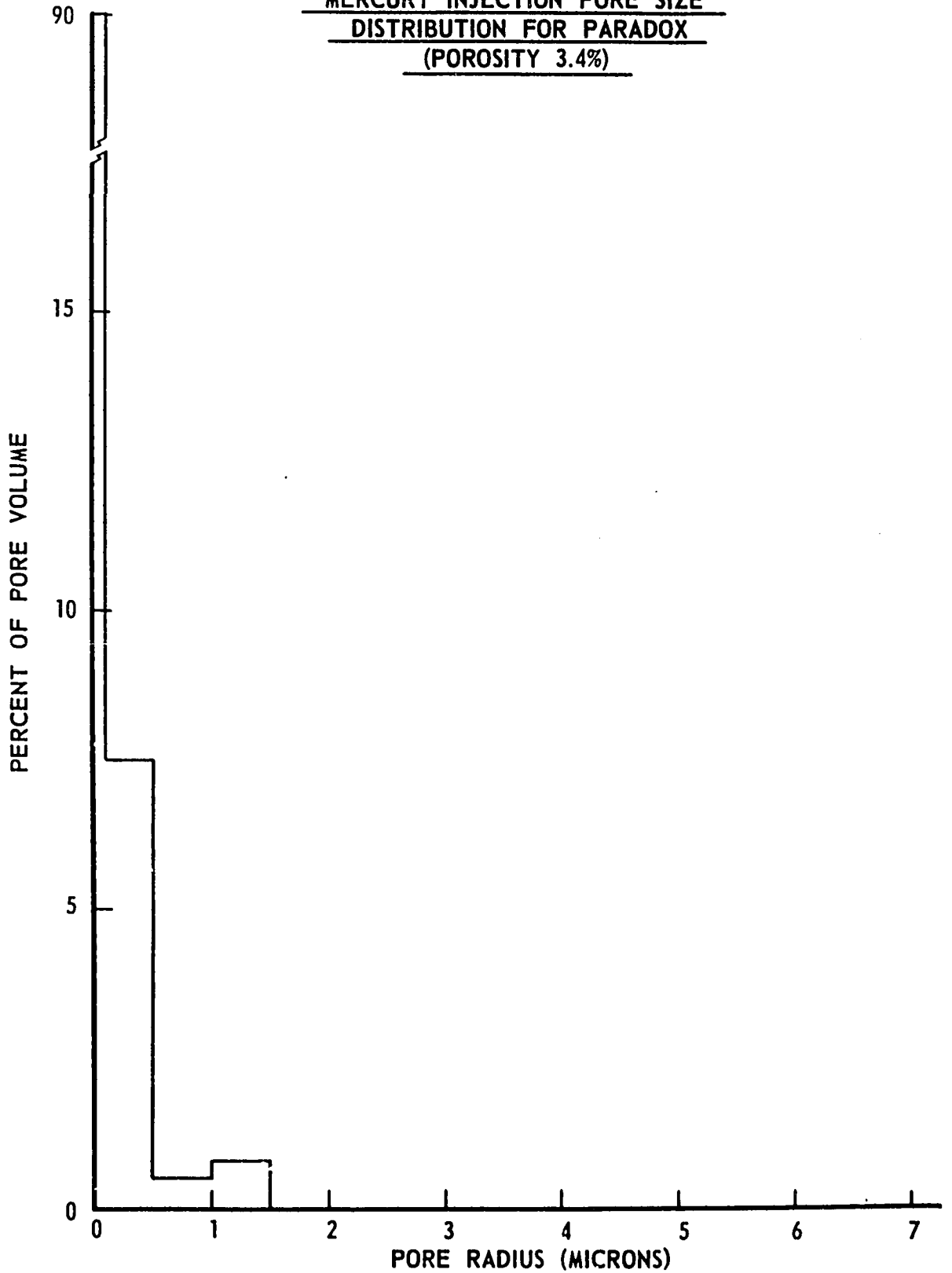




FIGURE 17  
MERCURY INJECTION PORE SIZE  
DISTRIBUTION FOR PARADOX  
(POROSITY 3.4%)

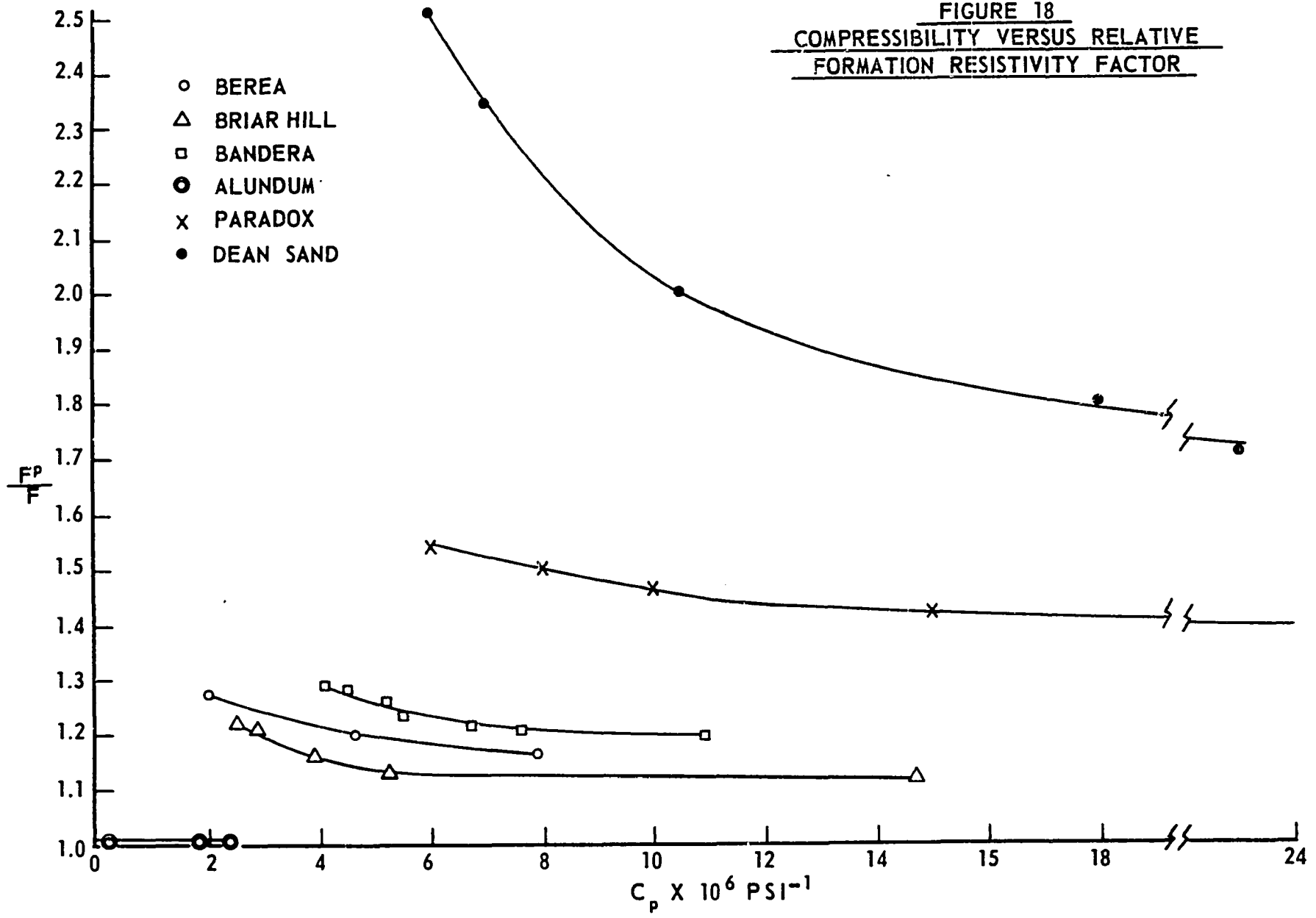


to establish correlations for most particular cases but a general correlation is evasive. One of the big problems is the lack of published rock properties for the pressure data available as well as the great variations in experimental procedures.

An attempt was made to verify the correlation of Dobrynin (Equation 1) but it was unsuccessful. One of the big obstacles was the correlation of pore compressibility with pressure. Above 500 psi. Dobrynin's data were linear on semilog graph paper but the data of the author (and also Knutson and Bohor<sup>18</sup>) were only linear for a very short interval. Ignoring this problem and forcing a curve fit to the data it was then impossible to find a correlation between Equation (1) and the data. The over-all problem is believed to be the great reliance of this method on the low pressure data, and the idealization of the pressure-compressibility relationship.

Some correlation between resistivity and pore compressibility may be possible (Figure 18) in special cases but as compressibility is a function of pore volume change and resistivity is more than just that, the intercorrelation is not a logical place to start. It should be noted that the pressure-compressibility curves presented by Knutson and Bohor are very regular and smooth for the quarry sandstones, but show definite character for the subsurface samples. This character (variation in direction and magnitude of the curve) may indicate that rocks have a "memory" and the irregular variations of compressibility, porosity, permeability, and resistivity may be some function of the subsurface stress conditions under which the sample was at equilibrium. It is quite possible that these subsurface

FIGURE 18  
COMPRESSIBILITY VERSUS RELATIVE  
FORMATION RESISTIVITY FACTOR



samples will be able to "tell us" more about the conditions existing below the surface than we can guess at. If this is so it may be possible to run a series of measurements and determine the actual permeability, porosity, resistivity, etc. the sample had in-situ as well as the stress conditions which would be of great value in our evaluation and stimulation techniques.

The fractional volume of small pores (i.e., with equivalent radii of less than 0.5 microns) appear to have some influence on the sensitivity of resistivity to overburden pressures as shown in Figure 19. The scatter of the data is rather wide but there does appear to be a general trend. The Alundum was used as an anchor point because of its very low fractional volume of pores less than 0.5 microns. At 1000 psi. net pressure all the data are relatively close to the curve while at 10,000 psi. the points are generally close to the curve with the exception of the Dean which has moved completely off the graph. The data used in this plot are summarized in Table III.

A good correlation between the relative formation resistivity factor at 1000 psi. and the clay content was obtained for the shale and shaly sands. For this correlation (Figure 20) the Briar Hill was assumed to have a clay content of approximately 2% which appeared to be reasonable. This relationship is not compatible with the clean formations such as the Paradox and Alundum because it assumes that the compressibility of the sand is a function of the shale content which implies that a clean formation would have very little if any response to pressure up to 1000 psi. which is not the case.

An examination of Figure 10 reveals that beyond a net pressure

**FIGURE 19**  
**PORE VOLUME <.5 MICRONS VERSUS**  
**RELATIVE FORMATION RESISTIVITY FACTOR**  
**AT 1000 PSI AND 10,000 PSI**

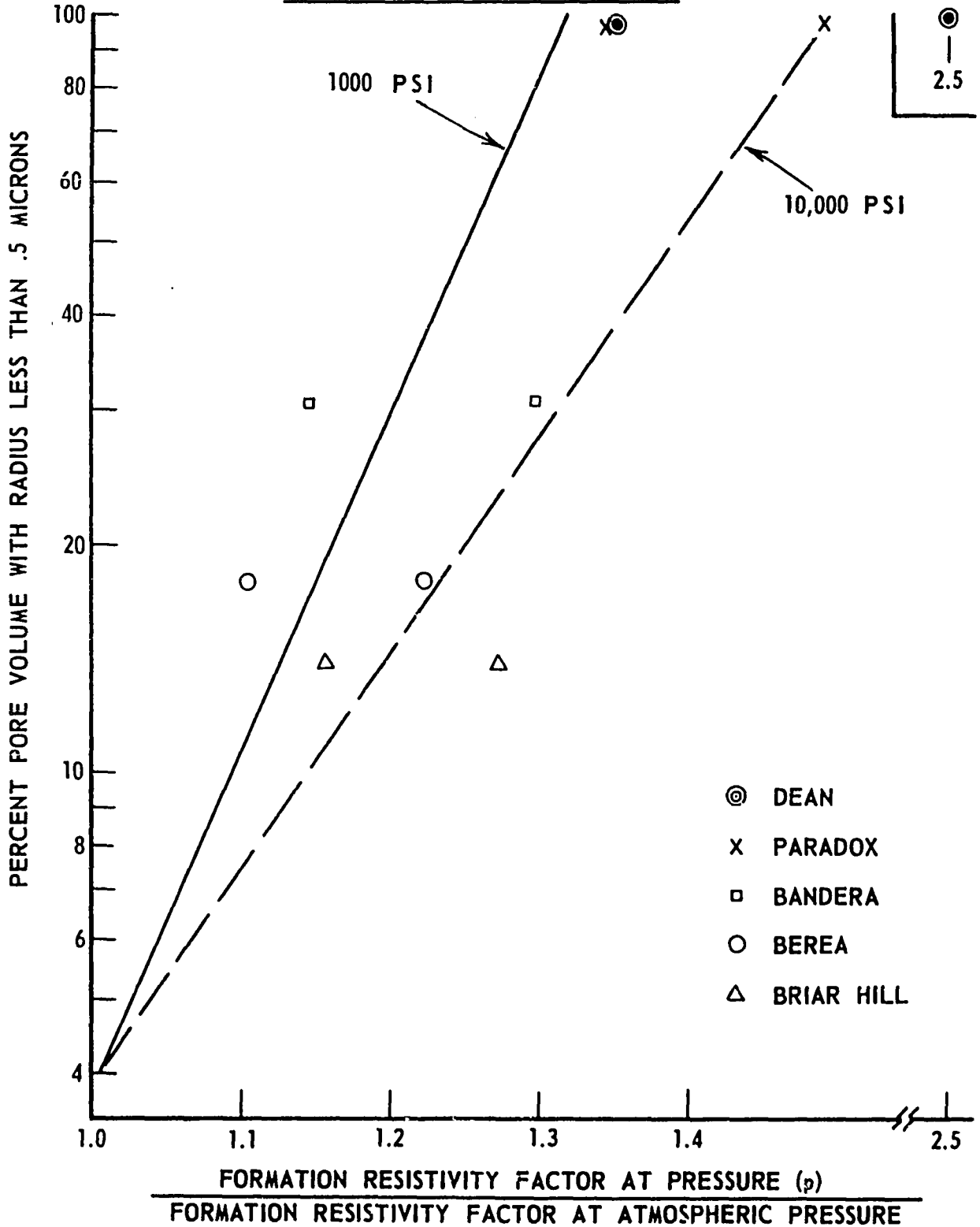


TABLE III

## SUMMARY OF THE EFFECTS OF PRESSURE

Sample	$\frac{F^P}{F}$		Percent Pore Volume With Radius		$\frac{\Delta\phi}{\phi}$	
	1000 psi.	10,000 psi.	<.5 m	<1 m	1000 spi.	10,000 psi.
Dean	1.35	2.51	97	97.5	.123	.264
Paradox	1.35	1.49	97.5	98	.47	.61
Bandera	1.19	1.30	31	38	.0475	.089
Berea	1.16	1.27	14	18	.048	.08
Briar Hill	1.11	1.22	18	23	.0435	.085
Alundum	1.005	1.005	4	6.5	.058	.064

m = micron ( $10^{-6}$  meters)

of 1000 psi. the data for the sandstones and limestone may be approximated by a straight line. The slope of this line for the sandstones ranges from 12.5 to 13 x 10<sup>-6</sup> psi.<sup>-1</sup> while for the limestone the slope is 21 x 10<sup>-6</sup> psi.<sup>-1</sup>. Two approximate relationships become immediately evident. The first is the combination of the percent shale correlation (Figure 20) and the constant slope for the shaly sands which is

$$\frac{F^P}{F} = 1.053 + .147 \log C + 12.5 \times 10^{-6} (P - 1000) \quad (13)$$

where C is the percent clay and P is the net pressure in psi. The second relationship is the combination of the pore volumes less than 0.5 microns at 1000 psi. and the straight line correlation above 1000 psi.

$$\frac{F^P}{F} = .868 + .225 \log (PV < .5) + A (P - 1000) 10^{-6} \quad (14)$$

where PV < .5 is the percent of pore volume of pores with equivalent radii less than .5 microns and A is a lithology constant of 12.5 for sands and 21 for limestone.

A graphical comparison of Equation (13) and the data are shown in Figure 21. The data are well represented by the equation as all the data are within 4% of the calculated values for pressures greater than 1000 psi. Equation (13) is very limited in scope and appears to be good for slightly to moderately shaly sands. It does not represent the shale which has a much greater slope. It may be possible to expand this correlation to more shaly sands with the availability of more data.

A graphical comparison of Equation (14) and the data is presented

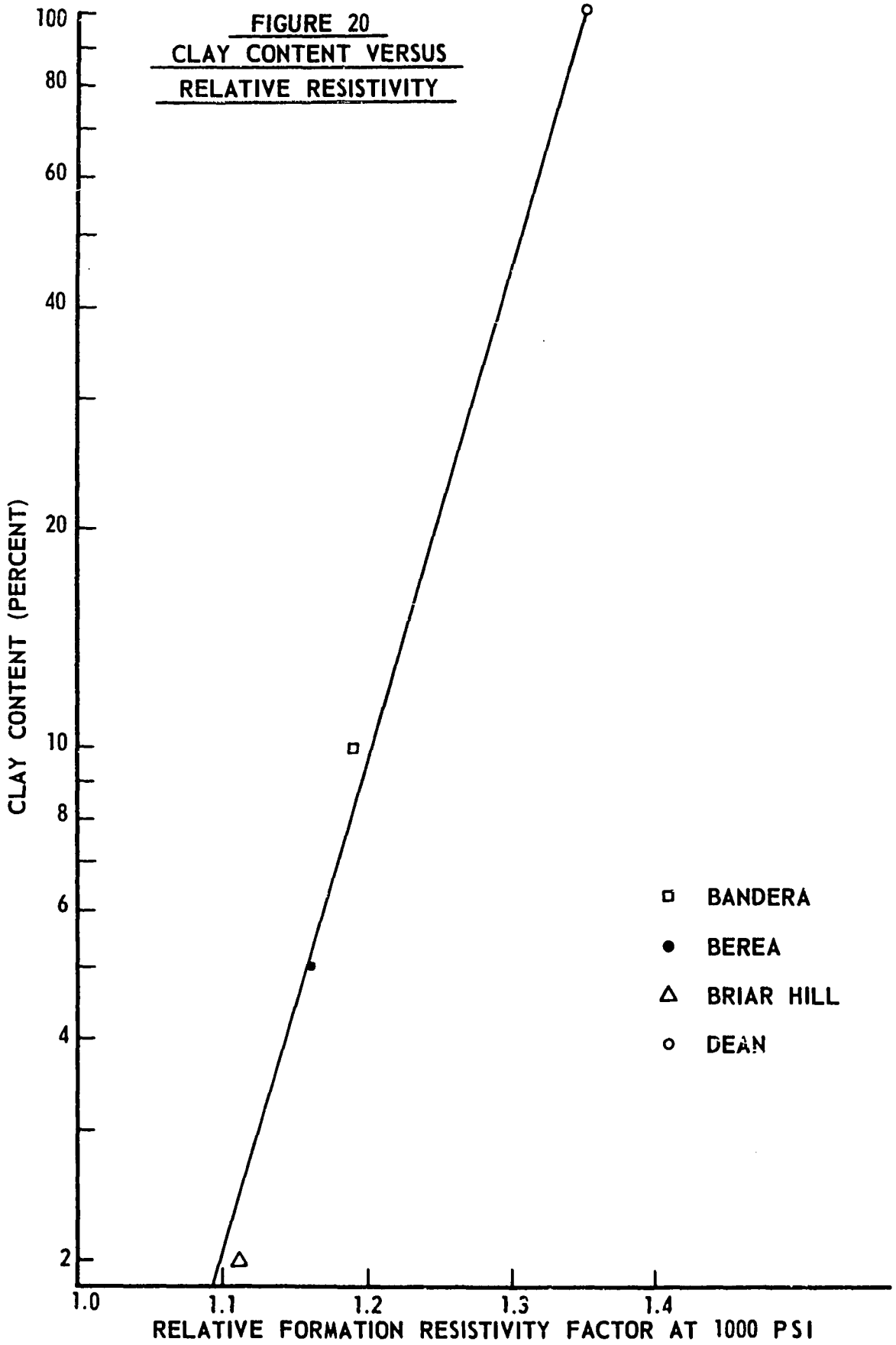
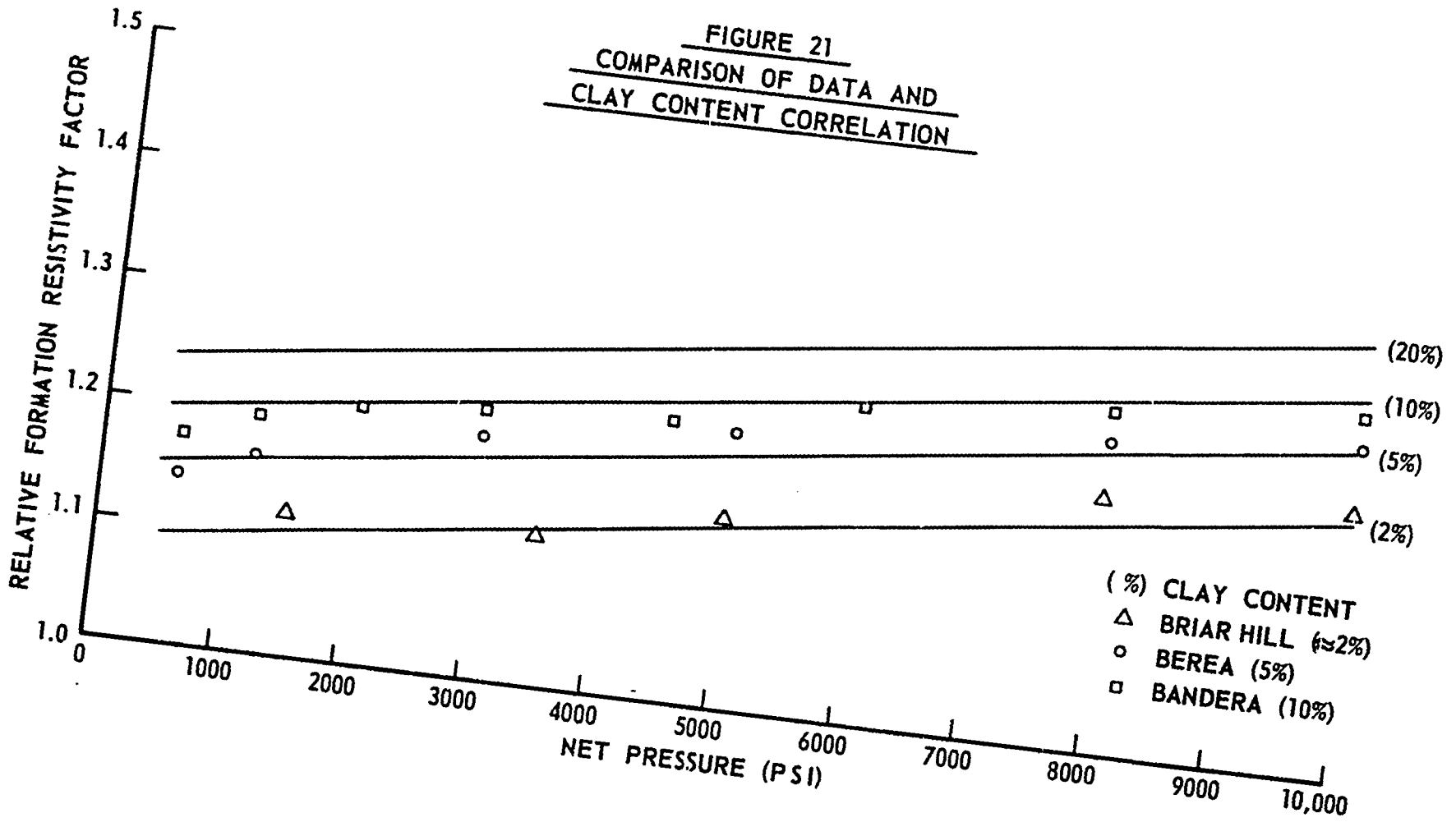




**FIGURE 21**  
**COMPARISON OF DATA AND**  
**CLAY CONTENT CORRELATION**



(%) CLAY CONTENT  
 △ BRIAR HILL (≈2%)  
 ○ BEREA (5%)  
 □ BANDERA (10%)

in Figure 22. The agreement is only fair with all the data within 10% and most of the data varying from 6 to 8% from the calculated values. Equation (14) is more general than Equation (13) but still does not represent the alundum response to pressure as the alundum increased very little beyond 1000 psi.

Neither of these two approaches should be considered more than an empirical way to obtain an approximate indication of the effect of net pressure, although this type of approach is very desirable because of the limited amount of data needed to obtain an answer.

For completeness, an analysis of the change in  $m$  ( $F = \phi^{-m}$ ) with pressure is presented in Figure 23. It is interesting to note that the three sandstones occupy approximately the same relative position they did in the relative Formation Resistivity Factor plot (Figure 10) while the limestone and alundum are transposed. The magnitude of the shale has been reduced. Unfortunately the variation in " $m$ " only indicates that the Formation Resistivity Factor is varying at the same rate, greater than, or less than the reciprocal of porosity to the  $m$  exponent. A closer look, using Owen's model as a guide, might imply that if  $m$  increases with pressure the constriction factor increases or the small pores are being decreased in radius more than the larger pores. A decrease in  $m$  would imply that the larger pores were being closed more than the smaller ones. The latter possibly indicates a pseudo viscous deformation as exhibited by the limestone. The shale would then be a combination of yielding and closing of small pores resulting in the decrease of separation

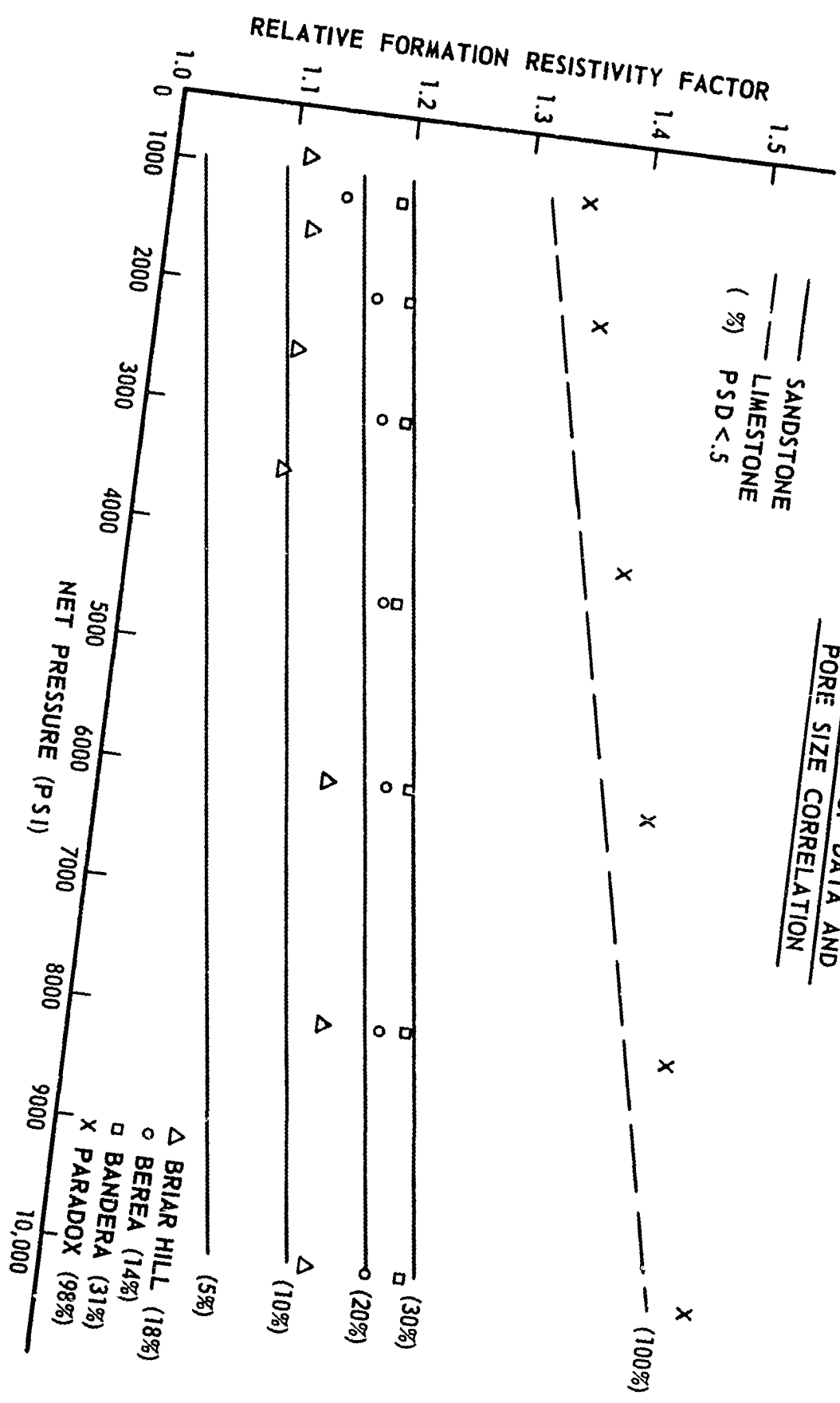
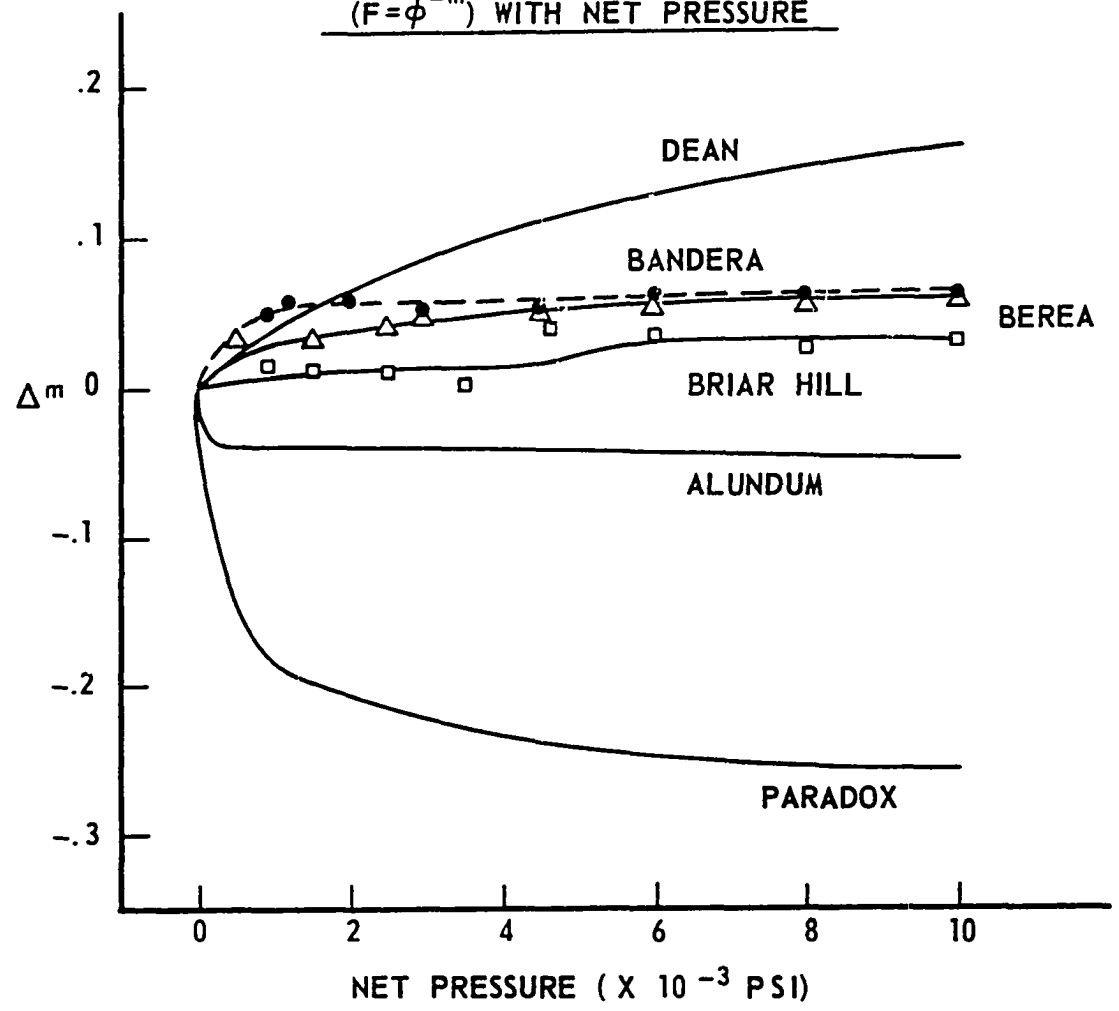


**FIGURE 23**  
**THE CHANGE IN  $m$**   
**( $F = \phi^{-m}$ ) WITH NET PRESSURE**



between the shale and the sandstones. The use of this type of analysis to fluid flow at overburden conditions might provide some interesting results.

The importance of knowing the effect of pressure on the Formation Resistivity Factor is not obvious until the routine use of subsurface measurements is examined. Archie's equation (10) is used in two ways in routine well log analysis. If porosity is required from a resistivity measurement an  $m$  factor must be available. These are generally determined at atmospheric conditions in a laboratory where the porosity and Formation Resistivity Factor are measured and  $m$  calculated ( $F = \phi^{-m}$ ). This may be best demonstrated with the Paradox laboratory data. At atmospheric conditions the Formation Resistivity Factor was 432.5 and the porosity was 2.82%. The  $m$  calculated from these values was 1.7. If we now assume that one of the measurements made under pressure (say 4000 psi.) was the value measured with a well log we have an  $F$  of 612.5. If we use the  $m$  of 1.7 calculated from the atmospheric data as is routinely done we obtain a porosity of 1.26% for an error of 82%.

In many cases in well log interpretation in-situ porosities are implied directly from subsurface measurements and it is necessary to convert them to a Formation Resistivity Factor to compare with resistivity measurements. Once more using the Paradox data and the calculated atmospheric  $m$  of 1.7 we will follow the routine used by log analysts. From one of our porosity tools we obtain a porosity of 1.26%. Using the  $m$  of 1.7 and  $F = \phi^{-m}$  we calculate an  $F$  of 1630. The calculated  $F$  is 174% greater than the measured value of 613.

The foregoing two examples indicate the large errors possible by not considering the effects of overburden pressure and in a small way indicate the need for a reliable means of converting between resistivity and porosity at in-situ conditions.

It is obvious that a more detailed work must be done on the effects of pressure on the resistivity of rocks taking into consideration such variables as pore sizes, composition, porosity, grain geometry, and other basic physical properties.

### TEMPERATURE

The variation of the relative Formation Resistivity Factor at constant effective stress and increasing temperature was generally the same for all samples. The relative Formation Resistivity Factor decreased from the initial value of 1, reached a minimum, and then increased as shown in Figures 24 to 26. The data for low (less than 2000 psi.) net stress can be represented generally as

$$\frac{F^T}{F} = G + \left[ \left( \frac{T}{100} \right)^{\frac{1}{2}} + \left( \frac{T}{100} - \alpha \right)^2 \right]^{\frac{1}{2}} A \quad (15)$$

where  $\frac{F^T}{F}$  is the relative Formation Resistivity Factor

T is the temperature in °F.

$\alpha$  is a variable which locates the minimum with respect to temperature.

A determines the magnitude of the minimum, and

G is a constant that normalizes each curve at the initial temperature.

The minimum relative Formation Resistivity Factor value is a function of the percent of pore volume represented by pores with a

FIGURE 24  
EFFECT OF TEMPERATURE ON  
RELATIVE RESISTIVITY OF BERA

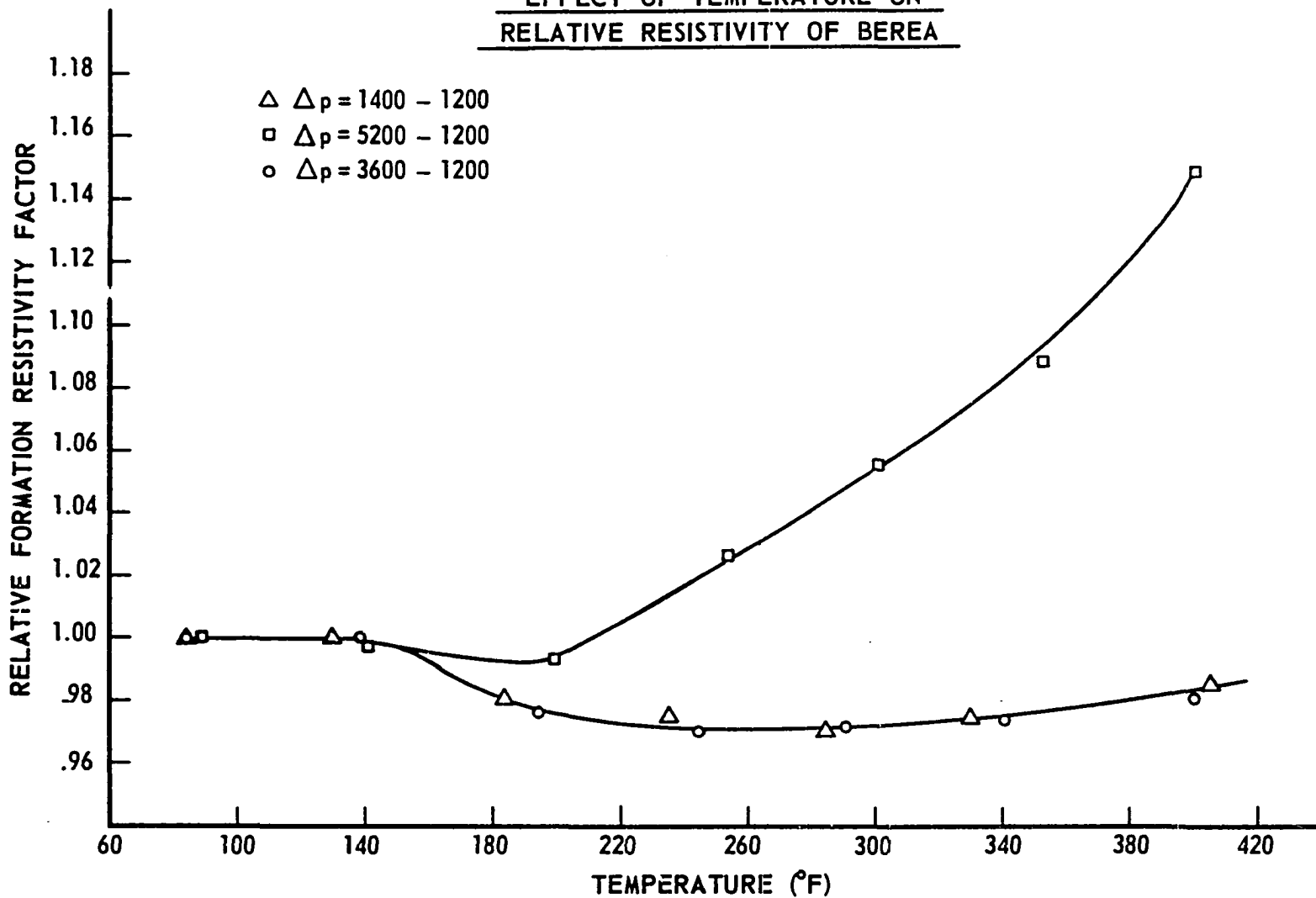


FIGURE 25  
EFFECT OF TEMPERATURE ON THE  
RELATIVE RESISTIVITY OF PARADOX  
AND DEAN SAMPLES

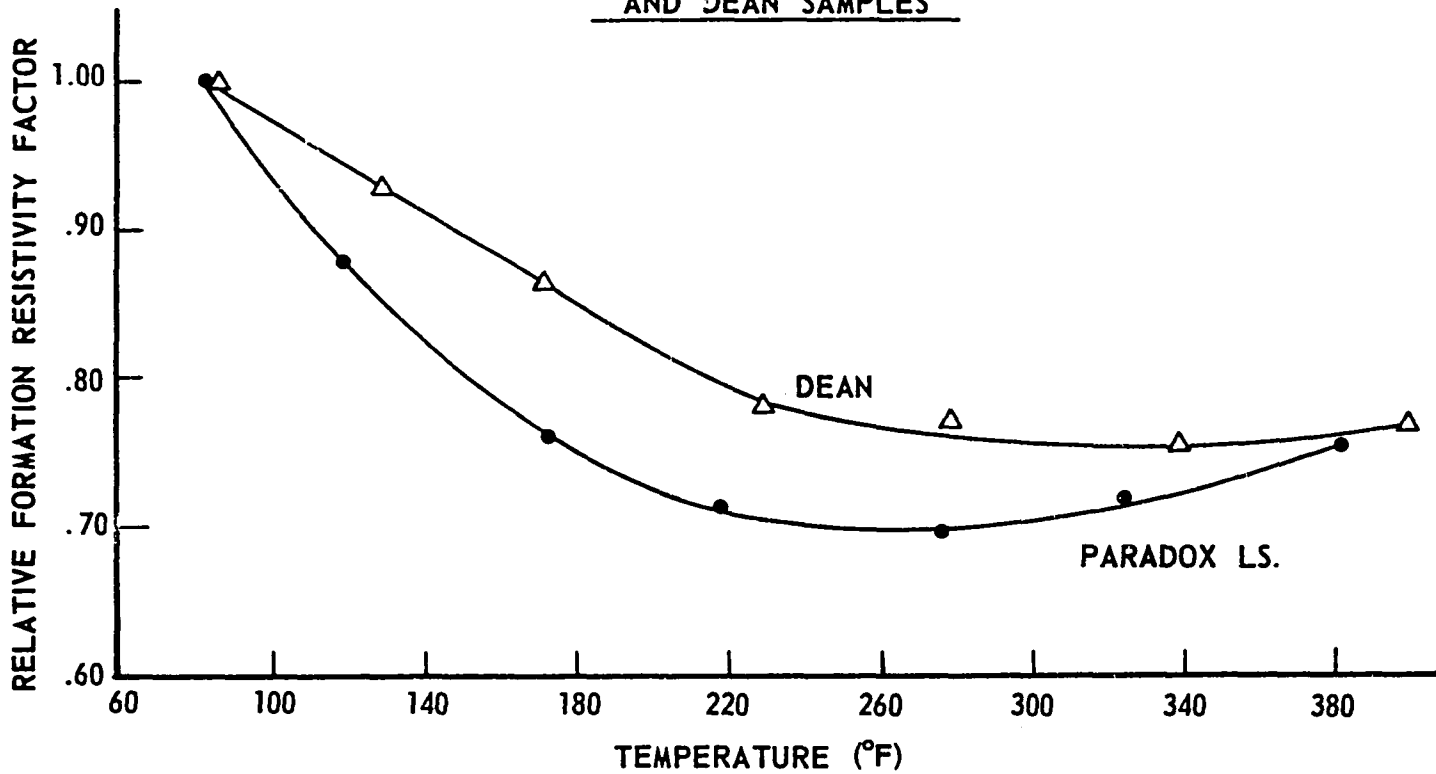
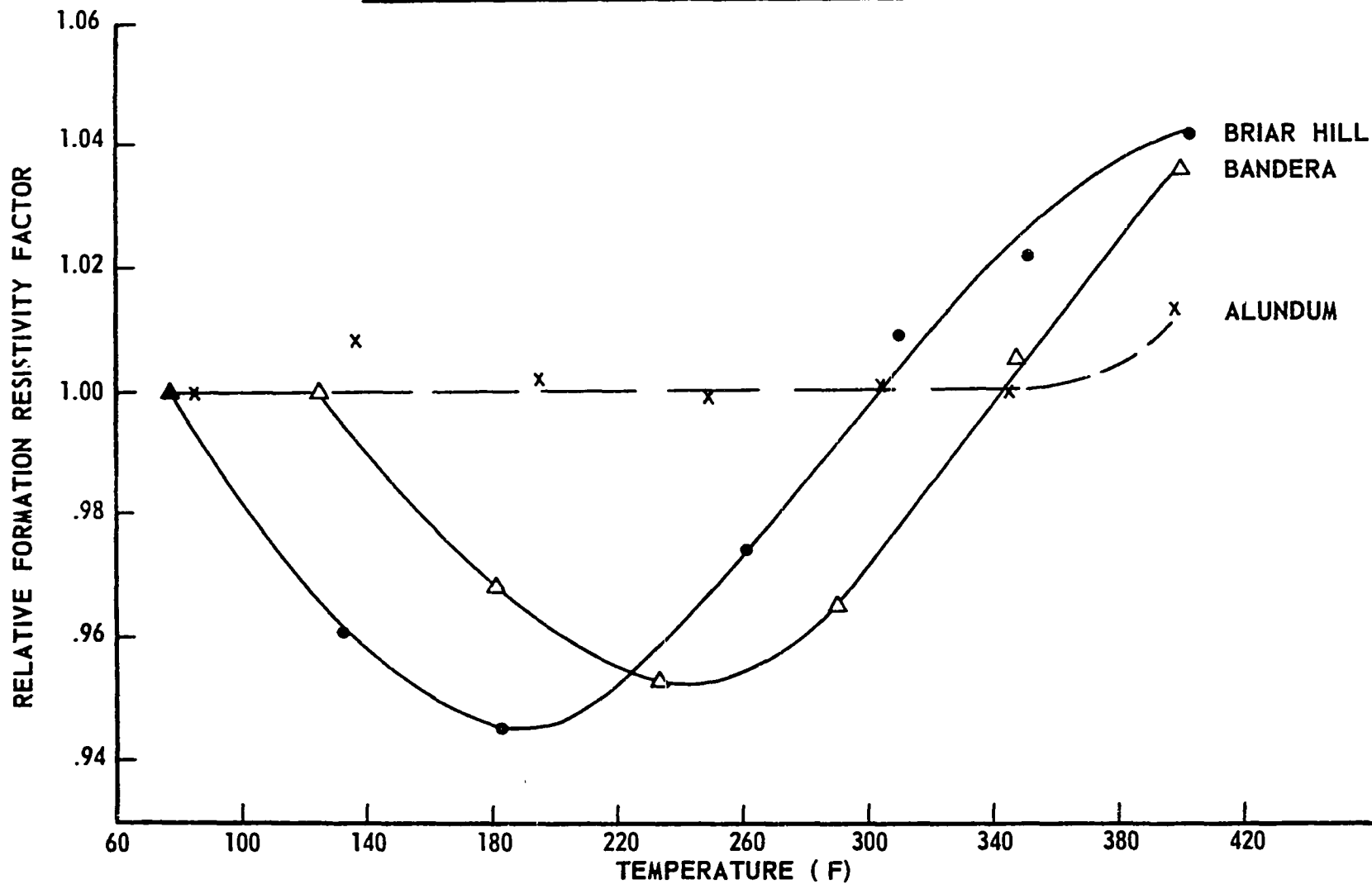




FIGURE 26  
EFFECT OF TEMPERATURE ON THE RELATIVE  
RESISTIVITY OF BRIAR HILL, BANDERA AND ALUNDUM



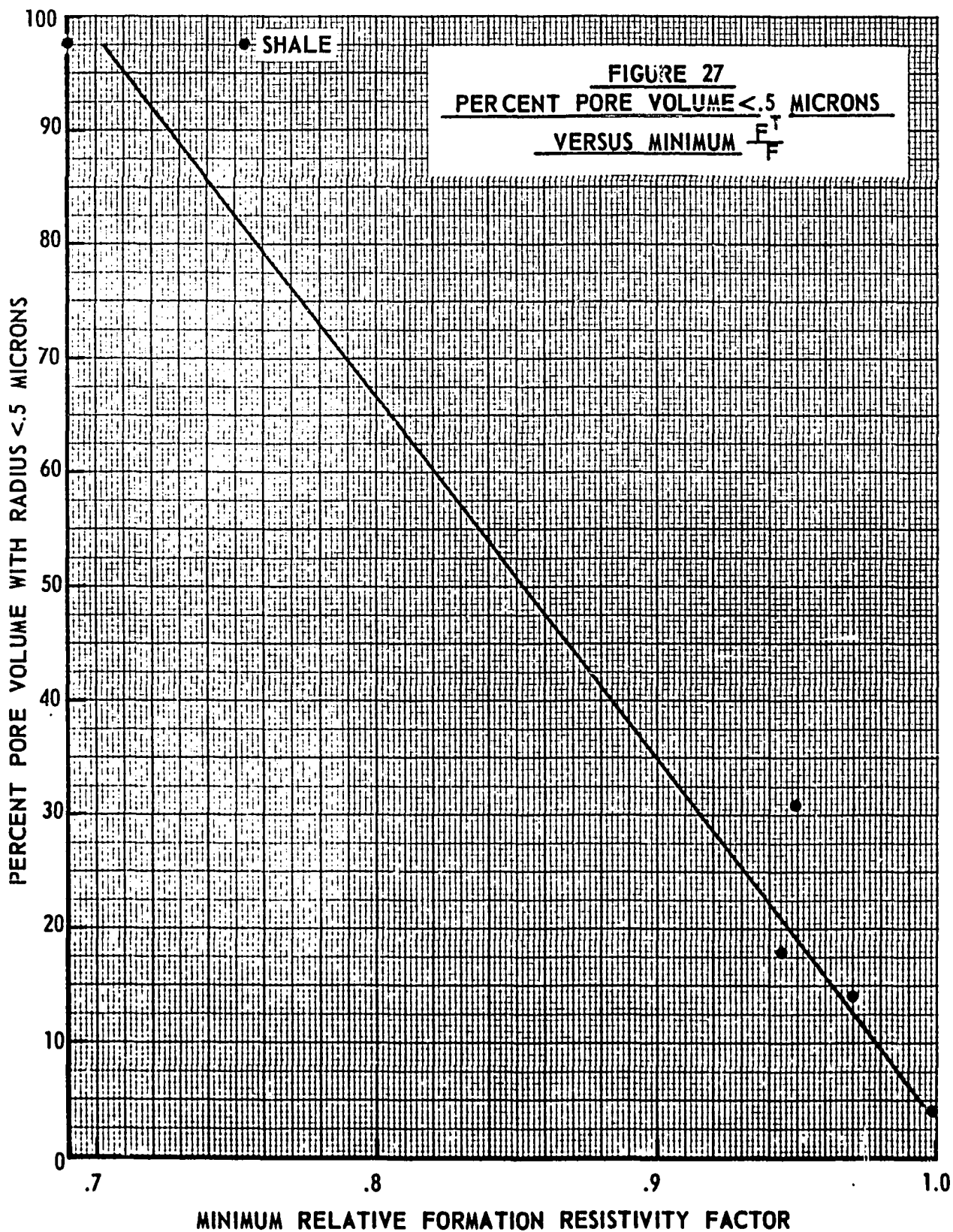
diameter less than 0.5 microns (hereafter referred to as the pores less than .5) as shown in Figure 27. It would be expected that "A" would be some function of the pores less than .5 microns. A correlation of "A" and the pores less than .5 microns for an  $\alpha$  of 2.9 is presented in Figure 28. Figure 29 shows the relationship between A,  $\alpha$ , and  $\frac{F^T}{F}$  minimum. The data were obtained by interpolation of the results of 40 series of calculations of Equation (15) for temperature from 80 to 400°F. It should be noted that the magnitude of the minimum relative Formation Resistivity Factor is not a function of temperature. The relationship between position of the minimum and  $\alpha$  is approximately

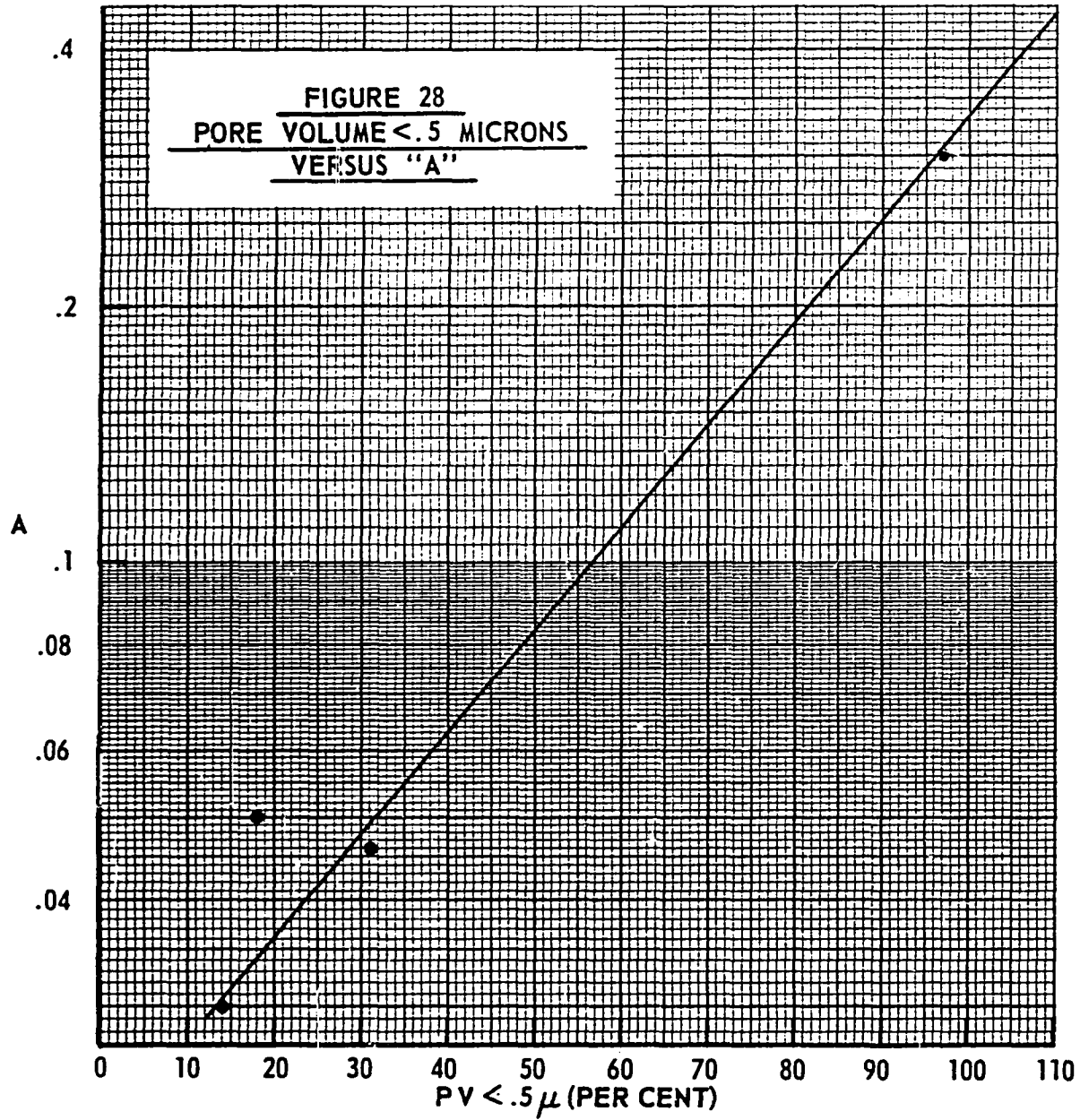
$$T_{\min} = 100 (\alpha - .2) \quad (16)$$

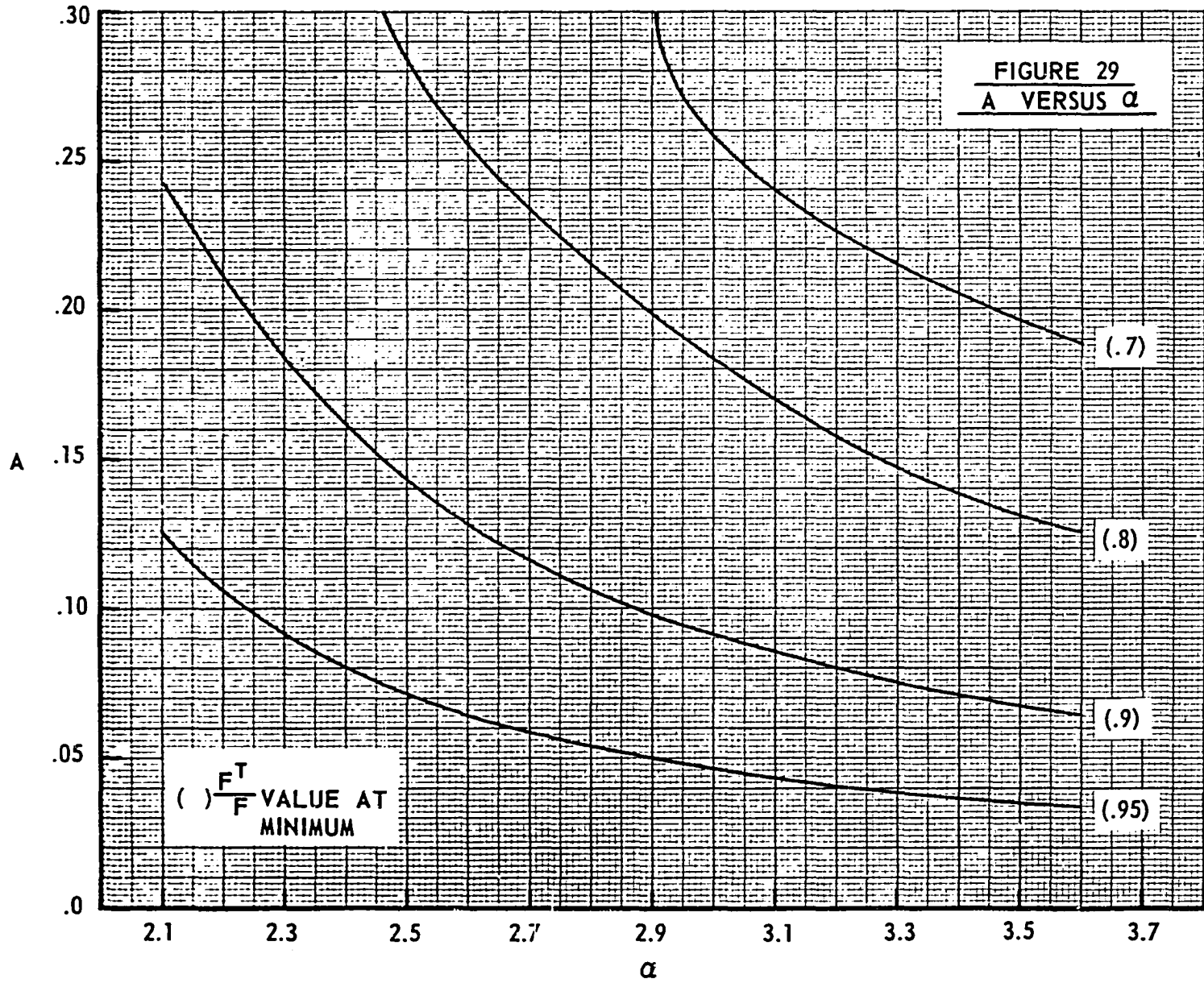
Using only the pores less than .5 microns some trial calculations were made to check the accuracy of the equation. Assuming an  $\alpha$  of 2.7 for the sandstones and 2.9 for the limestones, Table IV was calculated. For ease of discussion Equation (15) will be represented as

$$\frac{F^T}{F} = G + X. \quad (17)$$

A was first obtained from the pore size distribution and Figure 28 and then corrected to the appropriate  $\alpha$  using Figure 29. The initial A and  $\alpha = 2.9$  were located on this graph and then following parallel to the curves the point was shifted to the new A and  $\alpha$ . X was then calculated for a temperature of 80°F. G was determined as 1-X. Using this G,  $\frac{F^T}{F}$  was calculated for the desired temperatures between 80 and 400°F. The minimum  $\frac{F^T}{F}$  was obtained by varying







the temperature and recorded in Table IV. The calculated values of the minimum  $\frac{F^T}{F}$  are within 2% of the experimental values. Although some shift would be necessary to position the curves with respect to temperature the over-all correlation appears to be good. Figures 30, 31, and 32 show the comparison of the actual experimental data and the calculated data for the Paradox, Briar Hill, and Dean Sand for approximated  $\alpha$ 's. The agreement is good.

The decrease in the relative Formation Resistivity Factor is hypothesized as being the result of the thermal expansion of the rock grains causing the opening of the small pore diameters and thus reducing the resistivity in somewhat the reverse of what happens upon the application of pressure on the rock frame. The increase after the minimum is believed to be due to the thermal weakening of the cement binding the grains which closes the small pores again. The relative Formation Resistivity Factor of alundum did not vary appreciably with temperature which more or less eliminates the brine as the cause of the variation. The variation in water resistivity due to temperature and pressure does not appear to vary more than .5% from the variation of the water resistivity with temperature only. The existing data do not cover this case but this is believed to be a very close estimate. The shale content does not appear to be a major factor.

The behavior of the Dean Sand was not exactly the same as the other samples. The decrease in the relative Formation Resistivity Factor went through an abrupt change of slope at 230° and then went through a minimum at 340°F. It is believed that the shale is

TABLE IV

COMPARISON OF EXPERIMENTAL AND CALCULATED RELATIVE  
FORMATION RESISTIVITY FACTORS

Sample	PV (%)	$\leq .5$ ( $\infty = 2.9$ )	$\infty$	A	Calculated Minimum	Experimental Minimum
Berea	14	.03	2.7	.04	.97	.97
Paradox	97.5	.3	2.9	.305	.69	.69
Bandera	31	.049	2.7	.059	.95	.95
Briar Hill	18	.034	2.7	.044	.96	.945

FIGURE 30  
COMPARISON OF DATA AND CALCULATED  
RELATIVE FORMATION RESISTIVITY  
FACTOR FOR BRIAR HILL

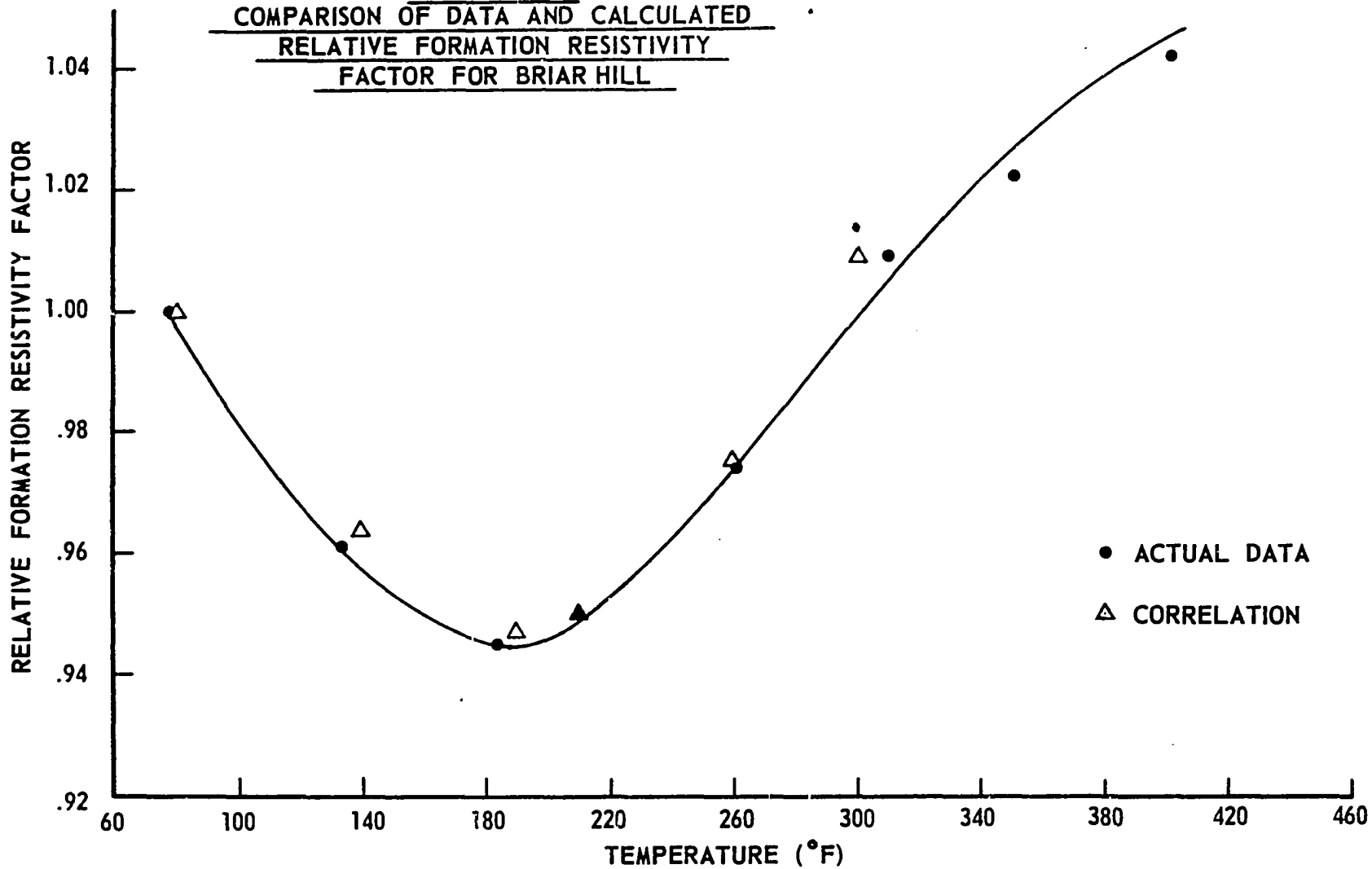




FIGURE 31  
COMPARISON OF DATA AND CALCULATED  
RELATIVE FORMATION RESISTIVITY  
FACTOR FOR DEAN

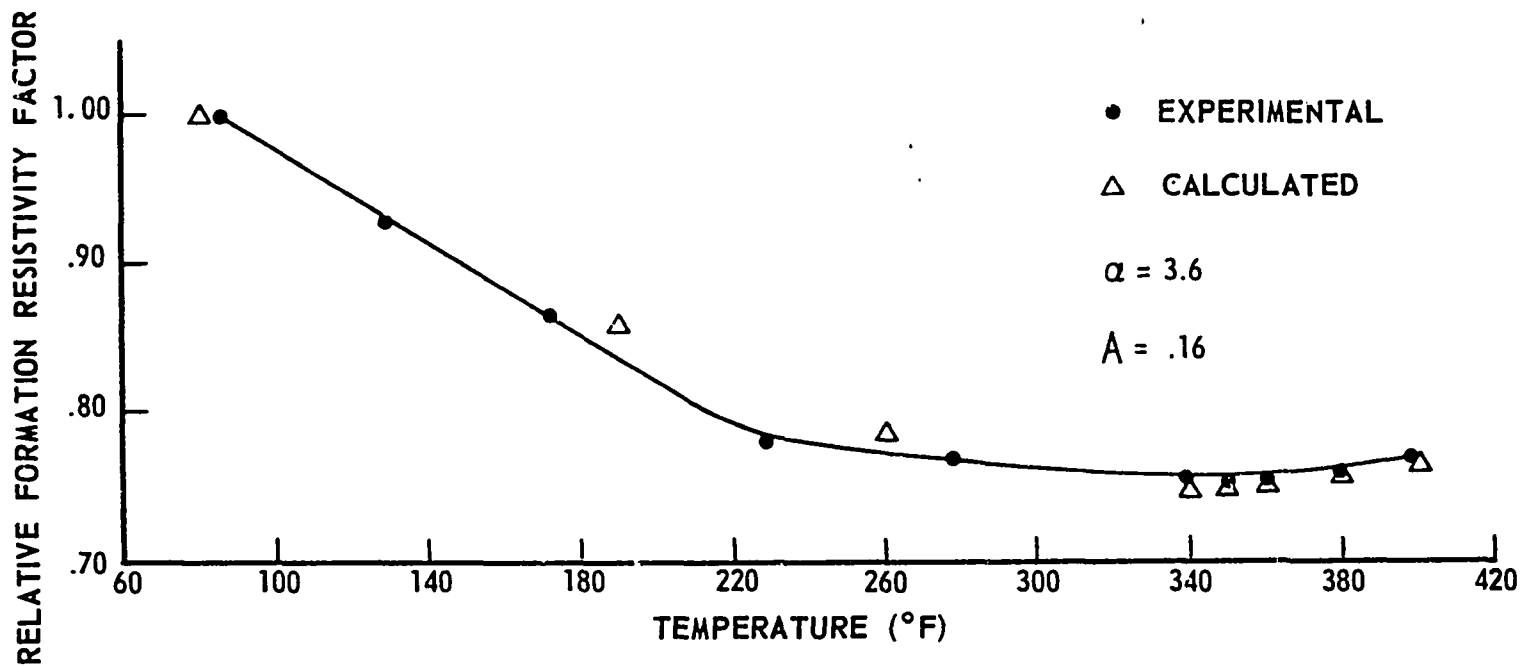
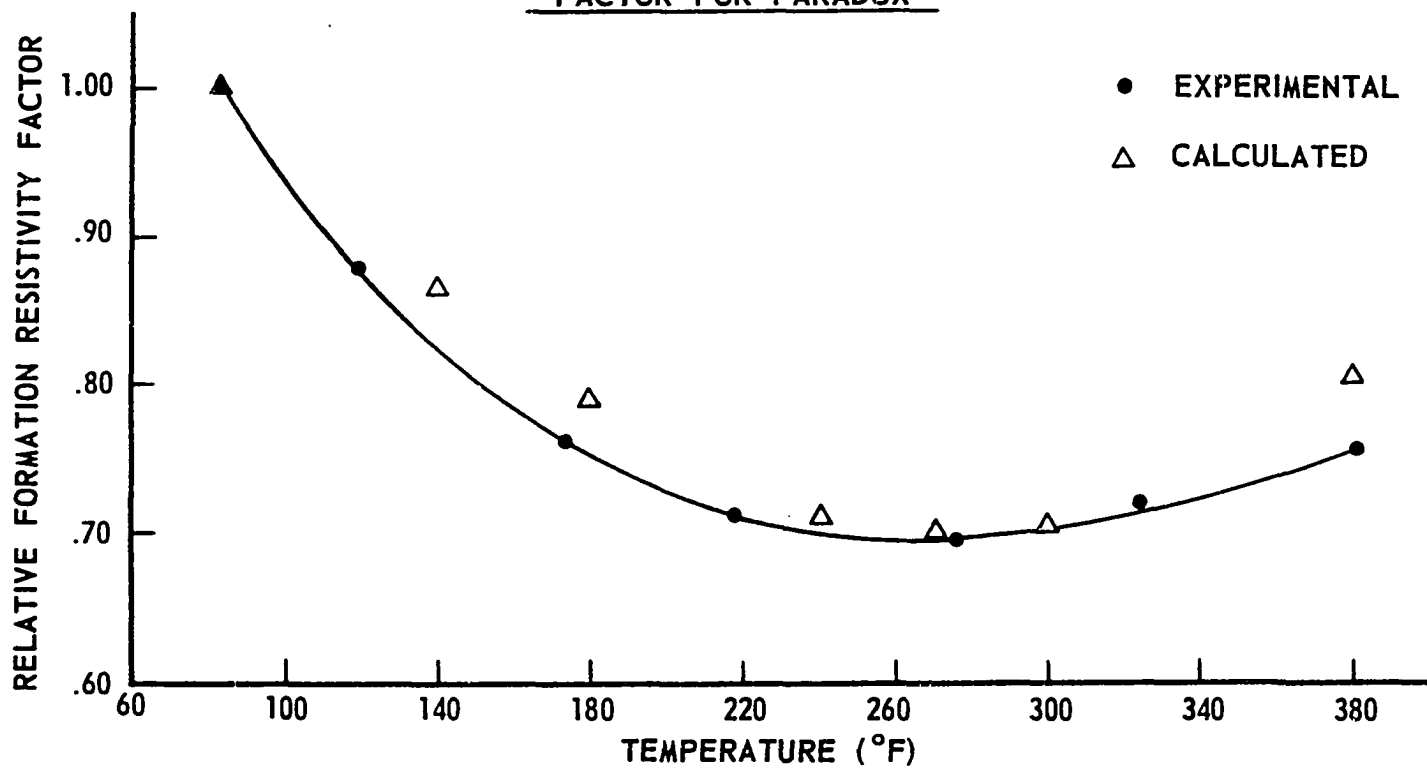


FIGURE 32  
COMPARISON OF DATA AND CALCULATED  
RELATIVE FORMATION RESISTIVITY  
FACTOR FOR PARADOX



experiencing the same minimum as the other samples but also a hydrating or dehydrating phase.

The  $\frac{F^T}{F}$  was measured for the Berea for effective stresses of 200, 2400, and 4000 psi. There was no change between the 200 and 2400 psi. data but there was an increase for the 4000 psi. data. The 4000 psi.  $\frac{F^T}{F}$  showed almost no minimum but increased 15% above the initial value. These data indicate that the rock deformed as a function of both temperature and pressure. It would appear that deformation occurs at high temperatures and low pressures, and at high pressures and moderate temperatures.

The absence of porosity data corresponding to the temperature data is unfortunate as it prevents any real quantitative diagnosis of the data. It does indicate that the change in resistivity is considerable in some cases and should be investigated for each particular case where laboratory data must be used as a calibration to facilitate interpretation of subterranean measurements.

#### PRESSURE-TEMPERATURE EXPERIMENTS

The results of the combined pressure-temperature experiments are shown in Figures 33 to 37 and are compared to composite pressure plus temperature curves obtained by the addition of the two independent sets of pressure and temperature data and normalized to a common beginning of 100°F. and/or 1000 psi. The normalization placed both curves (experimental and composite) at the same initial point to facilitate comparison. The agreement between the two curves is good with the exception of the Paradox which appears to be yielding. The 408°F. point for the Paradox was not an equilibrium point but was

**FIGURE 33**  
**EFFECTS OF TEMPERATURE PLUS**  
**PRESSURE ON ALUNDUM**

● EXPERIMENTAL

△ NORMALIZED PRESSURE PLUS  
TEMPERATURE DATA

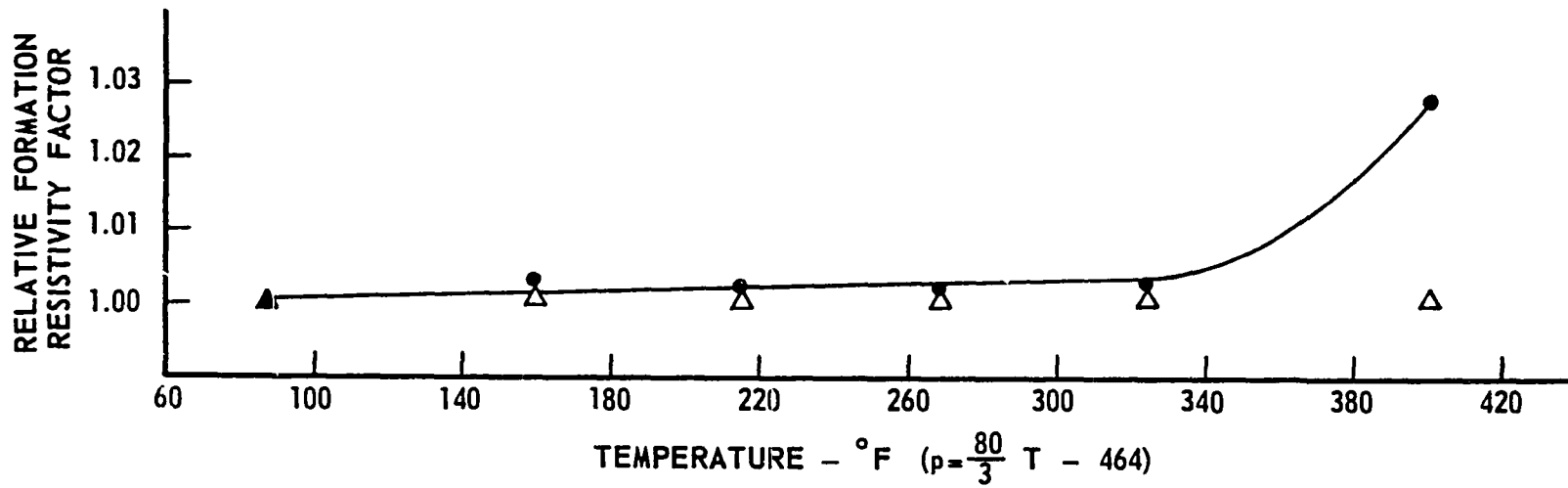


FIGURE 34  
EFFECTS OF PRESSURE PLUS  
TEMPERATURE ON BERA

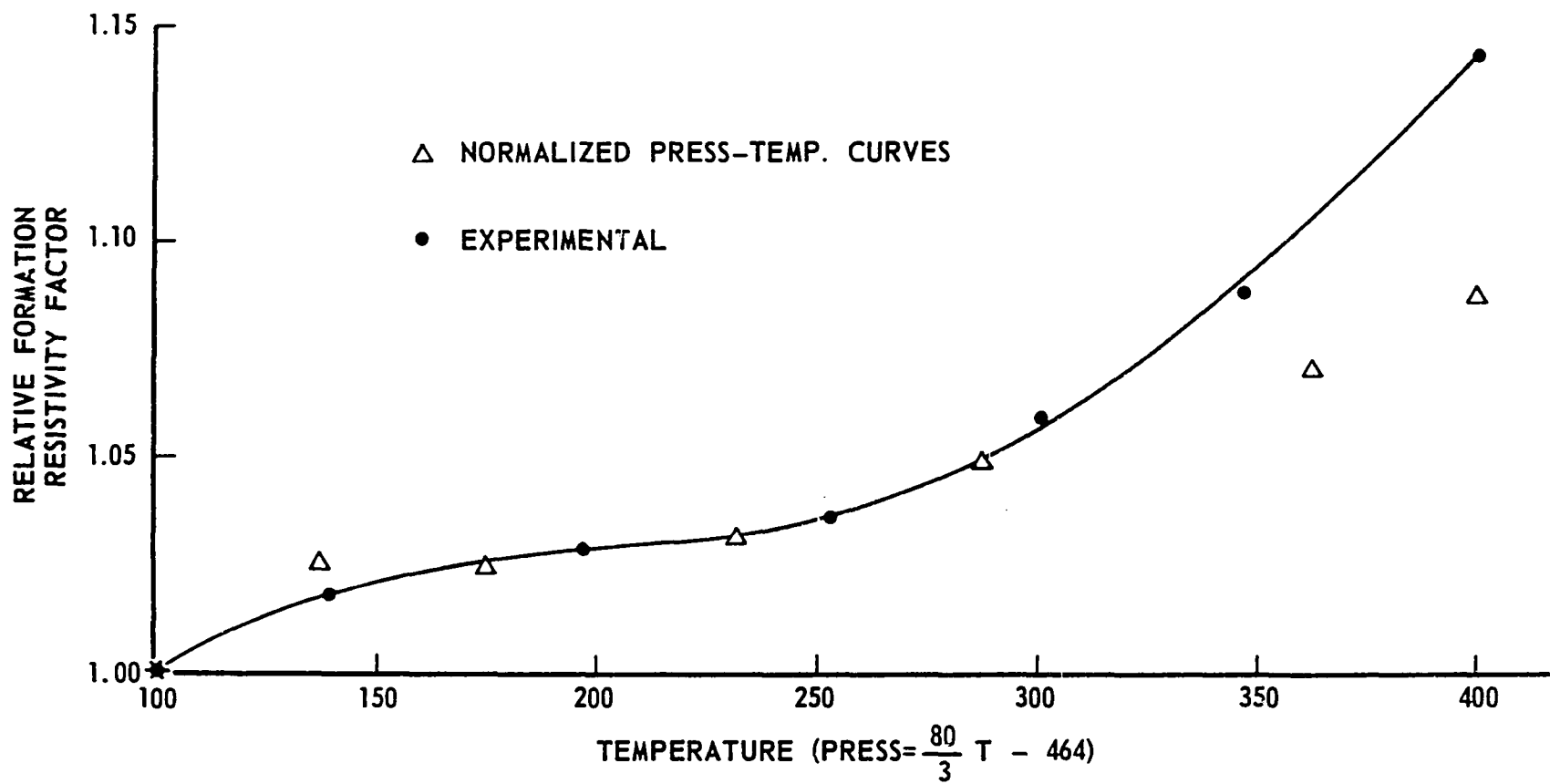


FIGURE 35  
EFFECTS OF TEMPERATURE PLUS  
PRESSURE ON BRIAR HILL

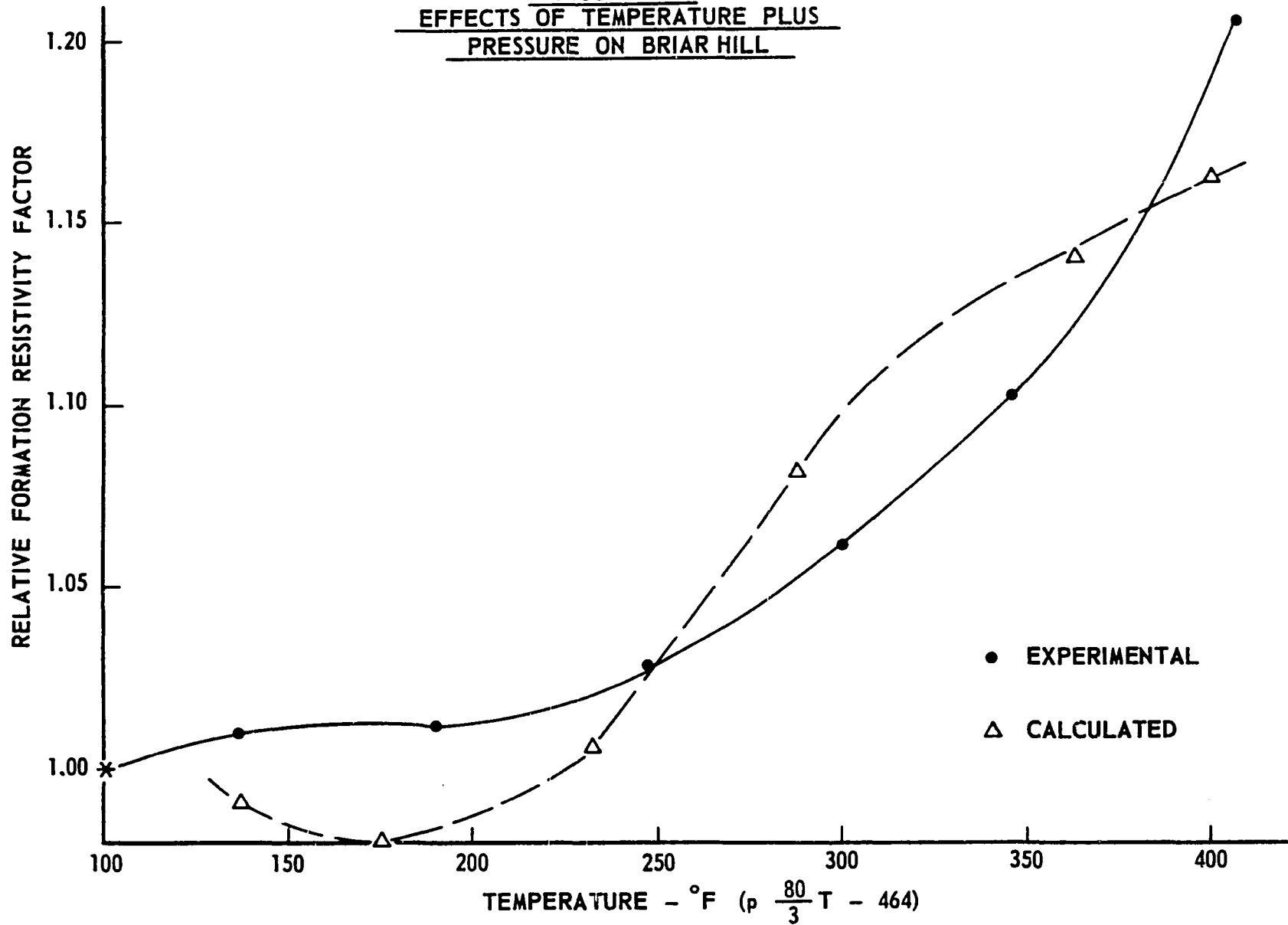


FIGURE 36  
EFFECTS OF TEMPERATURE PLUS  
PRESSURE FOR BANDERA

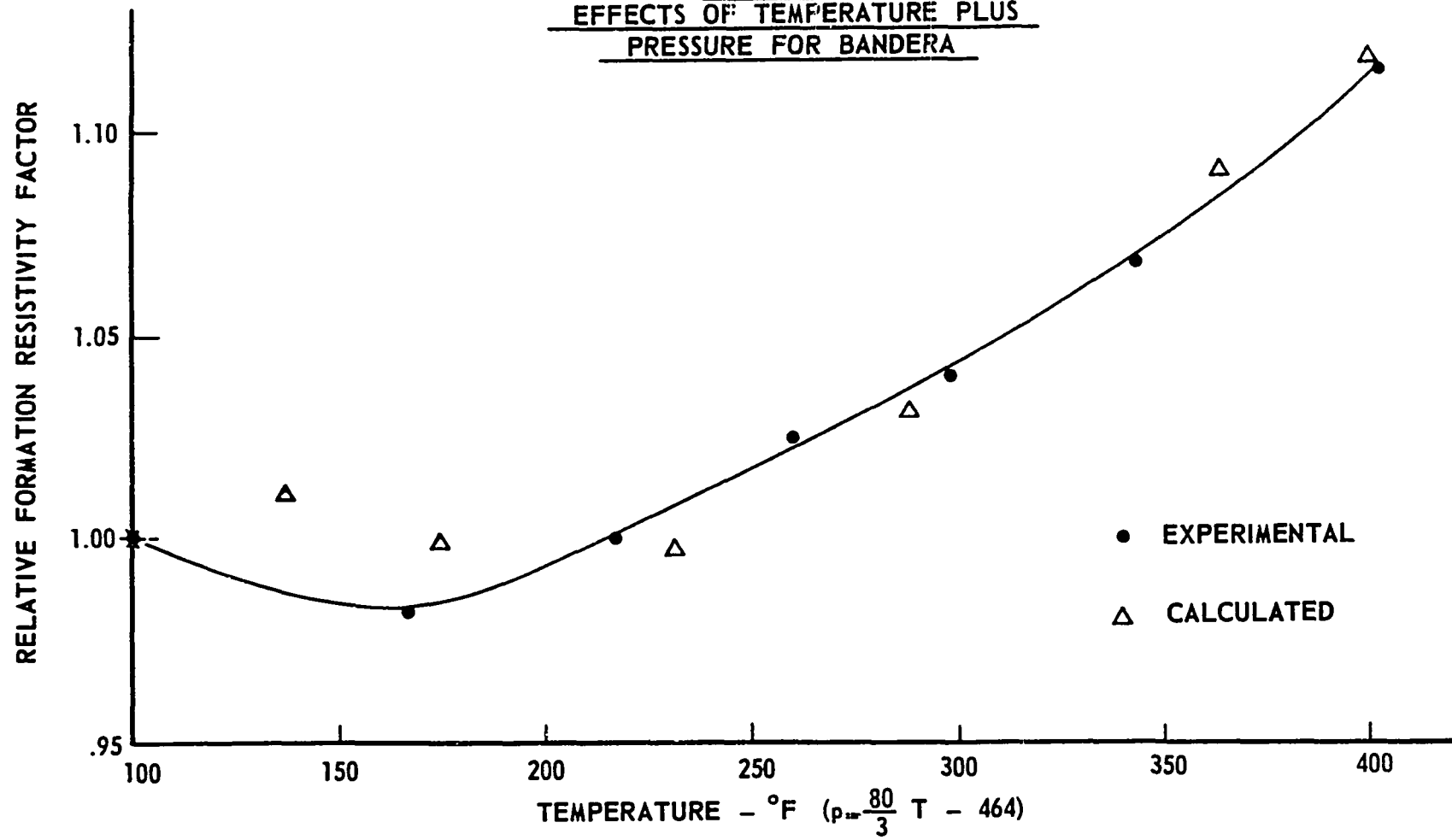
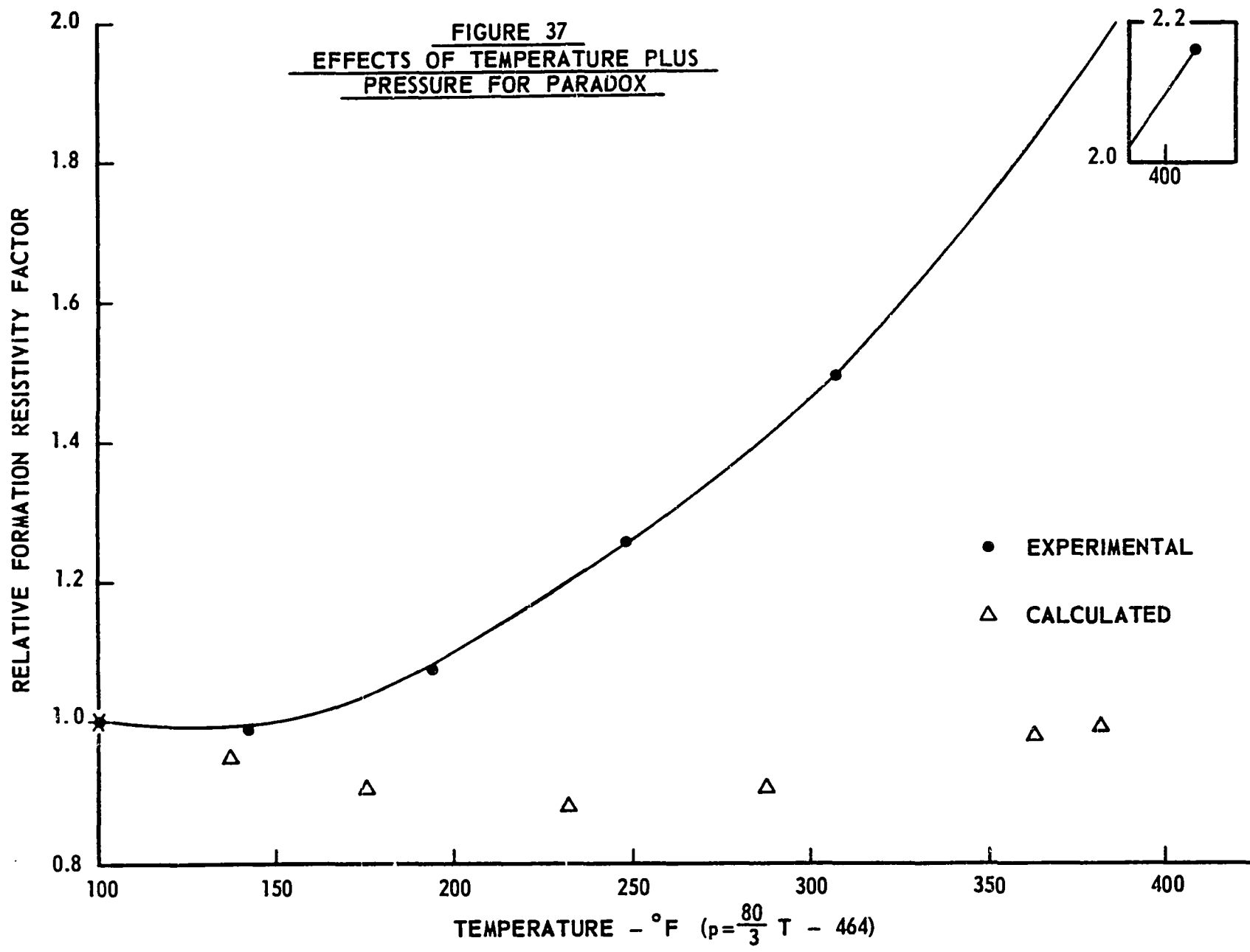


FIGURE 37  
EFFECTS OF TEMPERATURE PLUS  
PRESSURE FOR PARADOX





obtained four hours after the application of temperature and pressure when the resistivity was still changing rapidly and it became apparent that an equilibrium condition would not be obtained for a considerable time.

No pressure-temperature data were obtained for the Dean as equilibrium was not obtained within 36 hours after the first temperature and pressure increase. The manual operation of the equipment made waiting for equilibrium impractical.

In general the data indicate that the addition of the separate pressure and temperature data may be used to construct the effects expected by combined temperature-pressure experiments for the normal temperatures and pressures experienced by formations. This latter conclusion is not as important as it would have been before the development of a routine system of measuring the combined effects.

The deviations between the composite and the experimental data are considered to be caused by the "pseudo viscosity" of the samples. This yielding was noticed in all samples although the limestone and shale were the most pronounced. This pseudo viscous yielding of the limestone could account for the low matrix porosities of limestones and indicates the possibility of a correlation of matrix porosity and depth for limestones similar to that noticed by Athy<sup>3</sup> for shales.

## CHAPTER VI

### CONCLUSIONS

The measurement of physical properties at simulated overburden conditions are essential to improve analyses of porous media behavior demanded by advancing technology in the field of reservoir engineering. Electrical resistivity is one of the key properties as it is tied to the determination of the critically needed porosity and fluid saturation.

The first phase of this investigation was the development of a high pressure and temperature cell which made possible for the first time the measurement of rock resistivities at temperatures to 400°F. and/or pressures to 10,000 psi. This cell will, with only slight modifications, make possible the study of fluid flow through porous media under these same severe conditions.

The effect of increased temperature on the resistivity of formations is a function of the fraction of small pores with radii less than .5 microns and some unknown factor which locates the temperature at which the minimum occurs. Fortunately the minimum can be assumed closely enough for practical purposes once the rock type is known.

The sensitivity of the resistivity of formations to net pressure is among other factors a function of the volume of small pores and the clay content of the sample. No general correlation

is available at this time that will predict the effect of pressure on resistivity although a correlation of this type would be very valuable.

The effect of combined temperature and pressure on the resistivity of rocks is the sum of the separate temperature and pressure effects for low to moderate conditions. Above these conditions the formations tend to exhibit a pseudo viscous behavior.

Caution must be employed in generalizing the results obtained in this or any work to all consolidated porous media because it is never possible to investigate but a few representative samples. As this investigation has shown, there is wide variation in the resistivity of porous media and the manner in which it is affected by temperature and pressure.

**APPENDIX A**  
**SAMPLE DESCRIPTIONS**

## SAMPLE DESCRIPTIONS

- Alundum - manufactured porous medium normally used as water filters
- it is aluminum oxide
  - the homogeneity closely controlled
- Berea - quarry sandstone
- subarkose, fine grained sand
  - moderately well sorted
  - moderately hard
  - laminated
- Bandera - quarry sandstone (Bandera Stone Quarry, Redfield, Kansas)
- feldspathic, subgraywacke, very fine sandstone
  - moderately well sorted
  - soft competency
- Briar Hill - quarry sandstone (Briar Hill Stone Company, Glenmont, Ohio, Pottsville formation, Pennsylvanian Age)
- subarkosic, medium grained sandstone
  - moderately well sorted
- Dean - silty shale
- medium to dark grey in color
  - burial depth 8580 feet
  - burial temperature 135°F.
- Paradox - light grey limestone
- fine grained
  - burial depth 5900 feet
  - burial temperature 136°F.

APPENDIX B  
EXPERIMENTAL DATA

TABLE V

## VOLUMETRIC CHANGES DUE TO PRESSURE

Sample	Net Pressure (psi.)	Pore Volume (cm <sup>3</sup> )	Bulk Volume (cm <sup>3</sup> )	Porosity
Alundum A	0	14.427	54.558	.2644
	500	13.331	53.462	.2494
	1500	13.2898	53.4208	.2488
	2500	13.2598	53.3908	.2484
	4000	13.2353	53.3663	.2480
	6000	13.2138	53.3448	.2477
	8000	13.2032	53.3342	.2476
	10000	13.1943	53.3253	.2474
Bandera A	0	13.498	60.545	.2229
	100	13.156	60.203	.2185
	600	12.781	59.828	.2136
	1200	12.640	59.687	.2118
	2000	12.544	59.591	.2105
	3000	12.438	59.485	.2091
	4500	12.333	59.380	.2077
	6000	12.229	59.276	.2065
	8000	12.107	59.154	.2047
	10000	11.988	59.035	.2031

## VOLUMETRIC CHANGES DUE TO PRESSURE

Sample	Net Pressure (psi.)	Pore Volume (cm <sup>3</sup> )	Bulk Volume (cm <sup>3</sup> )	Porosity
Berea A	0	11.219	60.651	.1850
	100	10.9305	60.3625	.1811
	600	10.642	60.074	.1771
	1200	10.5465	59.9785	.1758
	2000	10.4745	59.9065	.1748
	3000	10.4035	59.8355	.1739
	4500	10.323	59.755	.1728
	6000	10.266	59.698	.1720
	8000	10.1965	59.6285	.1710
	10000	10.138	59.570	.1702
Briar Hill C	0	12.683	59.631	.2127
	300	12.2395	59.1875	.2068
	900	12.006	58.954	.2037
	1500	11.9042	58.8522	.2023
	2500	11.7762	58.7242	.2005
	3500	11.6852	58.6332	.1993
	4600	11.5967	58.5447	.1981
	6000	11.5215	58.4695	.1971
	8000	11.4235	58.3715	.1957
	10000	11.3420	58.2900	.1946



## VOLUMETRIC CHANGES DUE TO PRESSURE

Sample	Net Pressure (psi.)	Pore Volume (cm <sup>3</sup> )	Bulk Volume (cm <sup>3</sup> )	Porosity
Dean C	0	4.507	60.824	.0741
	300	4.173	60.49	.0690
	900	3.939	60.256	.0654
	1140	3.888	60.205	.0646
	1760	3.6908	60.0078	.0615
	2800	3.6118	59.9288	.0603
	4000	3.4763	59.7933	.0581
	6020	3.3856	59.7026	.0567
	7750	3.3071	59.6241	.0555
	10000	3.2471	59.5641	.0545
Paradox B	0	1.712	60.836	.02815
	1000	.8955	60.0195	.01493
	2000	.8163	59.9403	.01363
	4000	.755	59.879	.01262
	6000	.7275	59.8515	.01217
	8000	.679	59.803	.01135
	10000	.656	59.780	.01098

TABLE VI  
RESISTIVITY CHANGES DUE TO PRESSURE

Sample	Pressure	Temperature	Resistivity	F	$\frac{F^P}{F}$
Alundum A	0	104	.569	9.57	1.000
	500	103	.602	10.03	1.050
	1500	102	.611	10.02	1.049
	2500	104	.596	10.02	1.049
	4000	104.5	.5945	10.02	1.049
	6000	104	.5945	9.99	1.044
	8000	104	.598	10.05	1.051
	10000	104.5	.596	10.05	1.051
Bandera A	0	78	1.078	13.99	1.000
	100	78	1.231	16.00	1.143
	600	78	1.263	16.42	1.174
	1200	78	1.288	16.71	1.195
	2000	75	1.302	16.90	1.202
	3000	78	1.310	17.01	1.227
	4500	78	1.325	17.22	1.232
	6000	78	1.358	17.62	1.260
	8000	78	1.382	17.95	1.282
	10000	78	1.395	18.12	1.297

## RESISTIVITY CHANGES DUE TO PRESSURE

Sample	Pressure	Temperature	Resistivity	F	$\frac{F^P}{F}$
Berea A	0	76	1.172	15.55	1.000
	100	76	1.368	16.48	1.059
	600	76	1.472	17.75	1.141
	1200	76	1.482	17.85	1.148
	2000	76	1.528	18.42	1.185
	3000	76	1.550	18.68	1.200
	4500	76	1.575	19.00	1.222
	6000	76	1.599	19.28	1.239
	8000	76	1.622	19.55	1.259
	10000	76	1.643	19.80	1.272
Briar Hill C	0	79.5	1.111	14.72	1.000
	300	79.5	1.203	15.95	1.082
	900	79.5	1.228	16.27	1.104
	1500	79.5	1.242	16.45	1.118
	2500	79.5	1.250	16.55	1.123
	3500	79.5	1.250	16.55	1.123
	4600	79.5	1.342	17.80	1.209
	6000	79.5	1.320	17.49	1.188
	8000	79.5	1.342	17.80	1.209
	10000	79.5	1.358	17.99	1.221

## RESISTIVITY CHANGES DUE TO PRESSURE

Sample	Pressure	Temperature	Resistivity	F	$\frac{F^P}{F}$
Dean C	0	76	4.49	57.1	1.000
	300	78.5	5.02	65.6	1.15
	900	78.5	5.76	75.3	1.319
	1140	81	5.81	78.0	1.365
	1760	81	6.74	90.4	1.582
	2800	81	7.25	97.3	1.702
	4000	81	8.17	109.8	1.922
	6020	82	8.96	120.2	2.105
	7750	81	10.08	135.2	2.365
	10000	81	10.68	143.2	2.510
Paradox B	0	77	33.5	432.5	1.000
	1000	78	44.9	583	1.349
	2000	78.5	44.9	591	1.368
	4000	79	46.5	612.5	1.418
	6000	79	47.9	631	1.460
	8000	79	49.25	649	1.500
	10000	79	50.7	667	1.542

TABLE VII

## RESISTIVITY CHANGES DUE TO TEMPERATURE

Sample	Net Pressure	Temperature	Resistivity	F	$\frac{F^T}{F}$
Alundum B	2100-1100	85	.766	10.78	1.000
		137	.5055	10.87	1.008
		195	.3565	10.80	1.002
		248.5	.287	10.75	.998
		304	.2395	10.79	1.001
		344	.2175	10.78	1.000
		397.5	.200	10.92	1.013
Bandera C	2100-1100	76	1.275	16.37	1.000
		125	.819	16.35	.999
		180	.570	15.83	.968
		233	.4445	15.60	.956
		290	.368	15.80	.965
		347	.3335	16.47	1.006
		399	.3105	16.99	1.037

## RESISTIVITY CHANGES DUE TO TEMPERATURE

Sample	Net Pressure	Temperature	Resistivity	F	$\frac{F^T}{F}$
Berea #1	1400-1200	84	1.022	14.22	1.000
		129	.692	14.22	1.000
		183.5	.495	13.94	.981
		234.5	.3905	13.85	.975
		284	.328	13.79	.970
		330	.2905	13.85	.975
		405	.2485	14.01	.986
	5200-1200	88	.971	13.98	1.000
		140	.631	13.95	.9975
		199	.4565	13.89	.993
		253	.379	14.35	1.026
		300	.3305	14.57	1.055
		352	.304	15.20	1.088
		400	.292	16.05	1.148
Berea #3	3600-1200	84	1.149	16.08	1.000
		138	.740	16.08	1.000
		194	.527	15.70	.976
		244	.424	15.60	.970
		290.5	.366	15.63	.972
		340.5	.3205	15.65	.974
		400	.2870	15.78	.981

## RESISTIVITY CHANGES DUE TO TEMPERATURE

Sample	Net Pressure	Temperature	Resistivity	F	$\frac{F^T}{F}$
Briar Hill C	2100-1100	78	1.162	15.32	1.000
		133	.699	14.72	.961
		183	.514	14.48	.945
		261	.3815	14.90	.974
		310	.342	15.47	1.009
		351	.3125	15.65	1.022
		402.5	.289	15.97	1.042
Dean A	2100-1100	86	4.84	68.1	1.000
		129	3.045	62.5	.928
		172	2.16	58.9	.865
		229	1.535	53.1	.78
		278	1.270	52.4	.769
		339	1.052	51.3	.754
		398	.954	52.4	.769
Paradox A	2100-1100	82.5	47.6	649	1.000
		119	29.9	570	.878
		173	18.45	495	.762
		218	13.98	463	.713
		276	10.98	452	.696
		324	9.90	467	.719
		381	9.20	489	.754

TABLE VIII

## RESISTIVITY CHANGES DUE TO PRESSURE AND TEMPERATURE

Sample	Net Pressure	Temperature	Resistivity	F	$\frac{F^{PT}}{F}$
Alundum C	1900-1200	87	.705	10.07	1.000
	3800-1200	159	.405	10.10	1.003
	5300-1200	215	.3075	10.09	1.002
	6700-1200	268	.252	10.09	1.002
	7600-1200	324.5	.215	10.10	1.003
	10200-1200	400	.1893	10.35	1.028
Bandera B	2500-1200	111	1.079	19.10	1.000
	4000-1200	167	.721	18.75	.982
	5300-1200	217	.576	19.10	1.000
	6500-1200	260	.502	19.53	1.025
	7500-1200	298	.453	19.87	1.04
	8700-1200	343	.416	20.40	1.068
Berea #2	10200-1200	402	.386	21.3	1.115
	1900-1200	87	1.122	16.05	1.015
	3300-1200	139	.754	16.58	1.054
	4800-1200	197	.555	16.72	1.0575
	6300-1200	253	.444	16.88	1.068
	7600-1200	301	.3895	17.25	1.090
	8800-1200	347	.359	17.72	1.120
	10200-1200	400.5	.337	18.62	1.178



## RESISTIVITY CHANGES DUE TO PRESSURE AND TEMPERATURE

Sample	Net Pressure	Temperature	Resistivity	F	$\frac{F^{PT}}{F}$
Briar Hill A	1775-1200	84	1.143	15.79	1.000
	3200-1200	136.5	.75	16.13	1.022
	4600-1200	189	.559	16.18	1.024
	6100-1200	247	.444	16.42	1.040
	7500-1200	300	.3845	16.95	1.073
	8800-1200	346	.3565	17.62	1.117
	10400-1200	407	.345	19.28	1.220
Paradox C	1750-1200	83	11.98	164.2	1.000
	3300-1200	142	7.29	162.8	.992
	4700-1200	194	5.95	176.0	1.072
	6200-1200	248	5.52	206.0	1.255
	7700-1200	307	5.42	244.5	1.49
	10400-1200	408	6.36*	353.5	2.15

---

\* Did not reach equilibrium.

## BIBLIOGRAPHY

1. Adams, L. H. and Hall, R. E., 1931, "The Effects of Pressure on the Electrical Conductivity of Solutions of Sodium Chloride and of Other Electrolytes", Jour. of Phys. Chem., pp. 2145-2163.
2. Archie, G. E., 1942, "The Electrical Resistivity Log as an Aid in Determining Some Reservoir Characteristics", Trans. AIME, V. 146, p. 54.
3. Athy, L. F., 1930, "Density, Porosity, and Compaction of Sedimentary Rocks", Bull. Am. Assoc. Pet. Geol., V. 14, No. 1, p. 1.
4. Birch, F., 1942, "Handbook of Physical Constants", Geol. Soc. of Am. Spec. Paper No. 36.
5. Buchanan, J. and Hamann, S. P., 1953, "Chemical Effects of Pressure", Trans. Faraday Soc., V. 49, p. 1428.
6. Dakhnov, V. M., 1962, "Geophysical Well Logging", Quarterly of Colorado School of Mines, V. 57, No. 2 (translated by G. V. Keller from 1959 Russian edition).
7. Dobrynin, V. M., 1962, "Effect of Overburden Pressure on Some Properties of Sandstones", Soc. Pet. Eng. Jour., V. 2, No. 4, p. 360.
8. Fatt, I., 1957, "Effect of Overburden and Reservoir Pressure on Electrical Logging Formation Factor", AAPG Bull., V. 41, No. 11, p. 3456.
9. Fricke, H., 1924, "A Mathematical Treatment of the Electric Conductivity and Capacity of Dispersed Systems", Phy. Rev., V. 24, p. 575.
10. Geertsma, J., 1956, "The Effect of Fluid Pressure Decline and Volume Changes of Porous Rocks", AIME Paper 728-G.
11. Glanville, C. R., 1959, "Laboratory Study Indicates Significant Effects of Pressure on Resistivity of Reservoir Rocks", Jour. Pet. Tech., V. 11, No. 4, p. 20.
12. Giumov, I. F. and Dobrynin, V. M., 1962, "Changes of Specific Resistivity of Water Saturated Rocks Under the Action of Rock and Reservoir Pressures", Priklad. Geofiz., No. 33, p. 190.
13. Hall, H. N., 1953, "Compressibility of Reservoir Rocks", Trans. AIME, V. 198, p. 309.

14. Hughes, H., 1955, "The Pressure Effect on the Electrical Conductivity of Peridot", J. Geophys. Res., V. 60, No. 2, p. 187.
15. Hubbert, M. King, and Willis, D. G., 1957, "Mechanics of Hydraulic Fracturing", AIME Trans., V. 210, p. 153.
16. Long, G. and Chieici, G., 1961, "Salt Content Changes Compressibility of Reservoir Brines", The Pet. Engr., p. B-25.
17. Lynch, E. J., 1962, "Formation Evaluation", Harper & Row, New York
18. Knutson, C. F. and Bohor, B. F., 1963, "Reservoir Rock Behavior Under Moderate Confining Pressure", Fifth Symposium on Rock Mechanics, Pergamon Press Ltd., New York.
19. Maxwell, J. C., 1891, "A Treatise of Electricity and Magnetism", 1954 Reproduction, Dover Publications Inc., New York.
20. Orlov, L. I. and Gimaev, R. S., 1962, "The Influence of Rock Pressure on the Electrical Resistivity of Carbonate Rocks", Priklad. Geofiz., No. 33, p. 206.
21. Owen, J. E., 1952, "The Resistivity of a Fluid Filled Porous Body", AIME Trans., p. 195.
22. Pirson, S. J., 1947, "Factors Which Affect True Formation Resistivity", Oil & Gas Jour., Nov. 1.
23. Pirson, S. J., 1963, "Handbook of Well Log Analysis", Prentice Hall, Englewood Cliffs, New Jersey.
24. Rayleigh, Lord, 1892, "On the Influence of Obstacles Arranged in Rectangular Order Upon the Properties of a Medium", Phil. Mag., V. 34, p. 481.
25. Redmond, J. C., 1962, "Effect of Simulated Overburden Pressure on the Resistivity, Porosity, and Permeability of Selected Sandstones", PhD. Thesis, The Penn. State Univ.
26. Rust, C. F., 1952, "Electrical Resistivity Measurements on Reservoir Rock Samples by the Two-Electrode and Four-Electrode Methods", Trans. AIME, V. 195, p. 217.
27. Salwinski, A., 1926, "Conductivity of an Electrolyte Containing Dielectric Bodies", J. Chim. Phys., V. 23, p. 710.
28. Smith, L. B. and Keys, F. G., 1934, "The Volumes of Unit Mass of Liquid Water and Their Correlations as a Function of Pressure and Temperature", Proc. Amer. Acad. Arts and Sci., V. 69, No. 7.

29. Towle, Guy, 1962, "An Analysis of the Formation Resistivity Factor-Porosity Relationship of Some Assumed Pore Geometries", Proc. of Third Annual Symp. Soc. of Prof. Well Log Anal., Houston, Texas.
30. Winsauer, W. O. et al, 1952, "Resistivity of Brine Saturated Sands in Relation to Pore Geometry", Am. Assoc. Petr. Geol. Bull., V. 56, No. 2, p. 253.
31. Wyble, D. O., 1958, "Effect of Pressure on the Conductivity, Porosity, and Permeability of Oil Bearing Sandstones", PhD. Thesis, The Penn. State Univ.
32. Wyble, D. O., 1959, "Effects of Applied Pressure on the Conductivity, Porosity, and Permeability of Sandstones", Jour. Pet. Tech., V. 10, p. 57.
33. Wyllie, M. R. J. and Gregory, A. R., 1953, "Formation Factors of Unconsolidated Porous Media: Influence of Particle Shape and Effect of Cementation", Trans. AIME, V. 198, p. 103.
34. Wyllie, M. R. J., 1957, "The Fundamentals of Electric Log Interpretation", Second Edition, Academic Press, New York.
35. Wyllie, M. R. J., Gregory, A. R., and Gardner, G. H. F., 1958, "An Experimental Investigation of Factors Affecting Elastic Wave Velocities in Porous Media", Geophysics, V. 23, No. 3.